Doctoral Dissertations   Student Theses and Dissertations

Fall 2021

Complete experiments on multi-photon ionizations of ultra-cold and polarized atoms

Bishnu Prasad Acharya

Follow this and additional works at: https://scholarsmine.mst.edu/doctoral_dissertations

Part of the Atomic, Molecular and Optical Physics Commons

Department: Physics

COMPLETE EXPERIMENTS ON MULTI-PHOTON IONIZATION OF ULTRA-COLD

AND POLARIZED ATOMS

by

BISHNU PRASAD ACHARYA

A DISSERTATION

Presented to the Graduate Faculty of the

MISSOURI UNIVERSITY OF SCIENCE AND TECHNOLOGY

In Partial Fulfillment of the Requirements for the Degree

DOCTOR OF PHILOSOPHY

in

PHYSICS

2021

Approved by:

Daniel Fischer, Advisor
Michael Schulz
Paul E Parris
Ulrich Jentschura
Sanjay Madria

PUBLICATION DISSERTATION OPTION

This dissertation consists of the following two articles which have been submitted for publication, or will be submitted for publication as follows:

Paper I: Pages 20-38 are intended for submission to Physical Review A.

Paper II: Pages 39-56 are intended for submission to Journal of Physics B.

ABSTRACT

Fundamental atomic processes such as collision-induced ionization are of relevance in many scientific fields. Describing these reactions can still pose a substantial challenge due to the well-known "few-body problem", which entails that there is no analytical solution of the equations of motion for systems of more the 2 mutually interacting particle. Novel experimental tools and advancements in theorical methods enable to obtain detailed information on atomic dynamics providing insight into both, the phase as well as the amplitude of the quantum-mechanical wave functions of the particles. In this project, we developed experimental techniques studying multi-photon ionization of lithium in femto-second laser fields. A lithium target is prepared either in the polarized 2p (m_l = +1) state or in the un-polarized 2s ground state. The target is ionized in the laser field by the absorption of two, three, or four photons, and the energy and angular distributions of the emitted electrons are measured. For these relatively simple systems, several fundamental features are observed: First, polarizing the atoms before ionizing them changes the symmetry of the reaction and shifts in the photo-electron angular distributions are observed. This symmetry breaking process is called Magnetic Dichroism, and we explained it by the interference of partial waves with asymmetric distribution of magnetic sub-levels in the final state. Second, the experimental spectra are revealing violations of the lowest-order perturbation theory even at very low laser intensities, where this theoretical method is typically believed to describe the process well. This indicates that in many situations more advanced descriptions are required. And third, the simultaneous measurement of the ionization from the 2s and 2p states enables to extract final state phase information in a very intuitive way using a "double-slit" picture. The new results show very clean and fundamental realizations of quantum mechanical effects, and they help to improve our understanding of mechanisms and symmetries in light-matter interaction.

ACKNOWLEDGMENTS

TABLE OF CONTENTS

LIST OF ILLUSTRATIONS

SECTION

1. INTRODUCTION

One of the most intriguing concepts in quantum mechanics is wave-particle duality, which was postulated by Louis de Broglie in 1924 [1]. This concept implies that interference phenomena do not only occur for classical waves, but also for massive elementary or compound particles such as electrons or atoms, respectively. In the framework of the Schrödinger formalism, the state of particles (or systems of particles) is characterized by complex wave functions. Therefore, the complete quantum-mechanical information of such states do not only comprise the "real" amplitudes of the wave functions, which are directly observable in experiments, but also their "complex" phases, which – in many cases – are not directly accessible [2, 3]. Experiments, which provide all this information are regarded as a "complete" experiment [4, 5]. On the one hand, the data obtained in this type of experiments represent a very sensitive test for theoretical models that often rely on approximations or sophisticated numerical methods. On the other hand, understanding the phase-dependence on the detailed experimental parameters allows regulating it, thereby ultimately controlling the outcome of an experimental scheme. This is the basis of the field of "quantum control".

Photoreactions involving single atoms are ideally suited to perform this type of experiments, because these systems are relatively simple and there are numerous experimental tools which allow for some degree of coherence and phase control. The simplest conceivable process is single-photon ionization, which is generally dominated by electric dipole transitions and the according selection rules. Here the final state can be expressed in terms of interfering partial wave, each corresponding to a specific orbital angular momentum. It is straight-forward to show that extracting the complex phases of these partial waves requires the knowledge of the system's polarization either in the initial or in the final

state [6–9]. The first experiments of this type were reported by Heinzmann [10] as well as Heckenkamp and co-workers [11], who measured not only the angular distribution, but also the spin polarization of photo-electrons. In the following decades, further experiments on alkali as well as rare gas atoms were performed with novel experimental approaches and advanced tools, which allow to prepare the target atoms in polarized initial states, and such experiments are performed since almost 30 years (see e. g. [4, 12–16]).

More recently, the interest focused on multiphoton reactions where several photons are absorbed while promoting the electron to the continuum. Here, too, the absorption process is dominated by electric dipole transitions. Amongst other things, the effect of the relative polarization direction of the atom and the laser radiation was studied, which are particularly striking, if the atoms are ionized by circularly polarized light with the rotation of the lights electric field being either co-rotating or counter-rotating with the initially bound electronic current density [17, 18]. Differences in the electron angular and energy distributions as well as in the ionization rates for these two geometries are quantitatively measured in terms of the "circular dichroism" [18, 19]. At not too high intensities, the general features of such multiphoton ionization processes can qualitatively be understood already in a rather simple picture using the electric dipole approximation in the lowest-order perturbation theory (LOPT) [20]. Each absorbed photon of left- and righthanded circular polarization changes the magnetic sublevel of the atom by $\Delta m = -1$ or $+1$, respectively. For n being the minimum number of photons required to reach the ionization threshold, the final magnetic quantum number of the emitted electron's orbital angular momentum will be well-defined and $m - n$ or $m + n$, respectively, resulting in very different final states and ionization cross sections for the two relative helicities.

For linearly polarized light, the multiphoton ionization of an initially polarized atoms can be described much in the same way: If the electric field and atomic polarization vectors are perpendicular to one another, there are two possible changes Δm of the atomic

orientation, which are +1 and −1, resulting in an broad asymmetric m distribution of interfering final partial waves (i.e. $\langle m \rangle \neq 0$) ranging from $m - n$ to $m + n$. Surprisingly, experimental investigations for this situation are extremely sparse and, to our knowledge, limited to the case where a core hole is created in the ionization process while the polarization of the initial state is achieved by the excitation of a valence electron [21].

In the last 5 years, a novel experiment has been set up in the Physics Department at Missouri S&T. It combines three of the most advanced experimental tools available in atomic physics: First, a novel type of all-optical laser atom trap (AOT) [22] has been developed which enables to confine a large number of lithium atoms in a small volume (about 1mm diameter) in a vacuum chamber, cool it down to temperatures in the milli-Kelvin regime, and prepare it either in the atomic (2s) ground state or in the excited and polarized $2p(m_l = +1)$ state. Second, these atoms are then subjected to the intense laser radiation (up to 10^{13} W/cm^2) of an optical parametric chirped-pulse amplifier (OPCPA) which either can provide very short broad-band laser pulses (down to 5 fs with a spectral wavelength range between 600 and 1000 nm) or more narrow-bandwidth but longer pulses with tunable center wavelength. And third, after ionization of the atoms, recoil ions and emitted electrons are detected in coincidence measuring the three-dimensional momentum vectors in a "Reaction Microscope" – sometimes also referred to as cold target recoil ion momentum spectroscopy (COLTRIMS) [23, 24]. The combination of these three techniques is world-wide unique. It allows for a high level of control of the systems under investigation, and it enables to characterize the outcome of the reaction in great detail.

The first experiment performed with this setup was a complete single-photon ionization experiment [25]. Polarized lithium atoms were ionized by the absorption of a single photon from a pulsed, low-intensity Nd:YAG laser source operating at a wavelength of 266 nm. Photo-electron angular distributions (PAD) were measured using COLTRIMS. The

excellent resolution achieved in the experiment has allowed not only to extract the relative phase and amplitude of all partial waves contributing to the final state, but also enabled to characterize the experiment regarding target and spectrometer properties.

In a second series of experiments, the multiphoton ionization of lithium by circularly polarized light was investigated [19, 26]. The polarized lithium atoms exposed to a circularly polarized external field represents one of the simplest conceivable chiral systems. For a field frequency near the excitation energy of the oriented initial state (i.e. at a wavelength of 665 nm), a strong circular dichroism is observed and the photoelectron energies are significantly affected by the helicity-dependent Autler-Townes splitting. Besides its fundamental relevance, this system is suited to create spin-polarized electron pulses with a reversible switch on a femtosecond timescale at an energy resolution of a few meV. In a follow up study, the same effect for wavelengths varying between 665 nm and 920 nm was. Strong asymmetries were found and quantitatively analyzed. A very strong sensitivity on the center wavelength of the incoming radiation was observed. Overall, the co-rotating situation prevails. However, the counter-rotating geometry is strongly favored around 800 nm due to the 2p-3s resonant transition, which can only be driven by counter-rotating fields. The observed features provide insights into the helicity dependence of light-atom interactions, and on the possible control of electron emission in atomic few-photon ionization by polarization-selective resonance enhancement.

In the scope of the present thesis, multiphoton ionization for linearly polarized light was studied. Compelling results were obtained, revealing three interesting features which advance our understanding of multi-photon ionization. First, an angular shift for the ionization of polarized atoms is observed. For spherically symmetric or randomly oriented targets, the laser polarization direction represents a symmetry axis. This symmetry is broken for the ionization of Li(2p,m_l = +1) state electron. Similar effects have been observed in the tunnel ionization regime, where they are explained to be caused by the finite tunneling time of the active electron that translates into a shift of the mean emission angle due to

an angular streaking mechanism often referred to as 'attoclock'. In the presently studied multiphoton ionization regime, this asymmetry is regarded in terms of interfering partial waves with asymmetric m-distributions. Similar phenomena has been found for the absorption by ferromagnetic material and is referred to as Magnetic Dichroism (MD) [27]. Our observations are also consistent with earlier studies on electron [28] and ion impact [29].

Moreover, the details of the electron emission from the 2p state and observed a total number of six peaks in the PAD after absorption of two photons for 665 nm fs-laser beam. The number of peaks reflects the interference of partial waves with different magnetic quantum number m_l. Surprisingly, the observed number of peaks is in direct contradiction to the lowest-order perturbation theory (LOPT), where only four peaks are expected. More advanced theoretical methods have been used to describe that system in collaboration with theoretical groups and found that the calculation and experiment are in good agreement with LOPT violation.

Furthermore, for a wavelength of about 670 nm, the ionization of the 2s ground state can proceed either through the 2p($m_l = +1$) or 2p ($m_l = -1$) resembling a double-slit scheme. Here, the 2s ionization cross section corresponds to the interference of the waves from both slits, and the 2p ionization represents the emission of only one of the slits. Directly measuring ground as well as excited state ionization data allows to extract the interference term and, therefore, it provides information on the phase factors of the wave functions. Again, the extracted phases are in very good agreement with our theoretical model. Overall, the new observations deepen our understanding of light matter interaction, they provide insights into fundamental symmetries, and they help to develop and improve tools for the quantum control of atomic and sub-atomic particles.

2. MULTI-PHOTON IONIZATION OF ULTRA-COLD AND POLARIZED ATOMS

2.1. MULTI-PHOTON IONIZATION

The photo-electric effect is of tremendous historical importance for the development of quantum theory and it has led Einstein already more than hundred years ago [30] to postulate a light particle(photon) as flow of the photons is a wave, which was in direct contradiction to wave picture of light formulated within Maxwell's theory, which was generally accepted at the early 1900s. According to Einstein, each photon carries a certain amount of energy that depends on the wavelength of the light but not on its intensity. The observation of discrete energies of photo-electrons is then explained by the absorption of a single photon with an energy higher than or equal to the binding energy of the electron initially bound in an atom, molecule, or solid. With the development of more advanced and high-resolution light sources such as synchrotrons, the photo-electric effect became a widely used tool to probe atomic and molecular correlation and structure, and helped to shape our very detailed understanding atomic and molecular structure and processes. With the development of lasers starting in the 60s of the last century, very high field intensities became accessible which allowed to study non-linear processes where more than one photon are involved. A prominent example is multi-photon ionization (MPI) [31], where an electron is promoted to the continuum by absorbing more than one photon. Nowadays, optical intensities are attainable such that the electric field strength is equivalent to, or even surpass, the Coulomb-binding fields in atoms and molecules, if an intense laser pulses is focused into a volume analogous just slightly exceeding the magnitude of its wavelength [32]. In a simple picture, the ionization rate β_i in a multi-photon ionization process can be approximated by,

$$\beta_i = \sigma_n I^n \qquad (2.1)$$

where, I is the laser intensity, σ_n the total cross section of the process, and n the number of absorbed photons. In a simplistic picture, each absorbed photon increases the electron's energy, which populates transiently a (virtual) state, before it absorbs the next photon. The lifetime of the virtual state that is detuned from an eigenstate by Δv follows the Heisenberg uncertainty principle [33]. Because these lifetimes are generally very short, the photons need to be absorbed in a short time, and MPI is a strongly intensity dependent process. Figure 2.1 (left) shows the schematic of multi-photon ionization process.
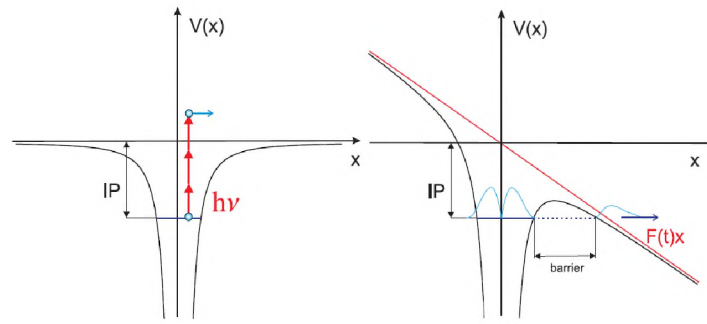
Figure 2.1. Multi-photon and tunneling ionization(From [34]): At low field intensities the ionization process proceeds through absorption of several photons. IP refers to the binding energy of the electron in the unperturbed atomic system.

Alternatively, the incoming light can be described in a classical field picture. Here, the initially bound electrons can be excited to the continuum through a tunnel ionization, i.e., the bound electron can pass through the potential barrier by the quantum-tunneling effect to become free. Generally, this semi-classical description of the ionization process represents a viable approximation, if the intensity of the laser field is very high and if the photon energy is small compared to the binding energy of the active electron. Quantitatively, the validitiy of either the multi-photon or the tunnel ionization picture is estimated by the Keldysh parameter γ [32, 35],

$$\gamma = \frac{\omega_L}{\omega_T} = \sqrt{\frac{W_P}{2U_p}}. \tag{2.2}$$

where, ω_L is the laser frequency, ω_T the characteristic tunneling rate, W_P the ionization potential, U_p is the ponderomotive potential which is equal to the time-average kinetic energy of a free electron oscillating in an ac field of intensity I. In atomic units, The ponderomotive potential is given by $U_p = \frac{I}{4\omega_L^2}$. For $\gamma > 1$, the ionization process is well described in the multi-photon picture, while for $\gamma < 1$ corresponds to the tunneling ionization regime.

2.1.1. Above Threshold Ionization (ATI). In the non-linear regime, an electron bound to an atom or molecule absorbs multiple photons, in some cases even more than are required to exceed the ionization threshold. This phenomenon is known as "above threshold ionization" (ATI). In this case, peaks in the photo-electron spectrum appear at energies

$$E_s = (n + s)\hbar\omega - W_p \qquad (2.3)$$

where, the integer n represents the minimum numbers of photons absorbed, the integer s represents the number of additional photons absorbed, ω is the angular frequency and W_P the ionization potential [36]. The multi-photon absorption could also be followed by the radiative decay of the electron back to an atomic bound state, resulting in the emission of a higher-energetic photon, whose frequency is an odd harmonic of the exciting field. This process is known as optical harmonic generation (OHG) [37, 38].

2.1.2. Resonance Enhanced Multi-Photon Ionization (REMPI). Another phenomenon occurring in non-linear photoreaction is "resonance enhanced multi-photon ionization" (REMPI). It involves the transient resonant excitation to an electronically excited intermediate atomic eigenstate state which is followed by the absorption of more photons ionizing the atom [39, 40]. This resonant eigenstate typically increases the probability of the multiphoton absorption and, hence, the ionization cross section.
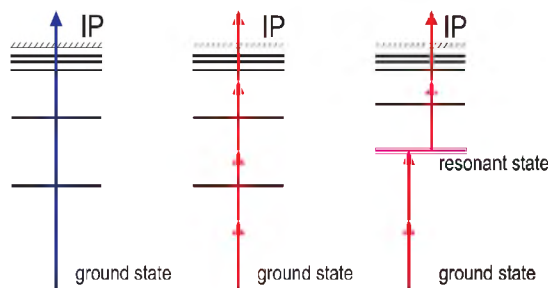
Figure 2.2. Photoionization of an atom (Picture taken from [34]), left to right: Single photon ionization,multiphoton ionization (MPI) and Resonance enhanced multiphoton ionization (REMPI).

Figure. 2.2 shows a schematic diagram of a REMPI process in which the molecule in the initial state absorbs two photons to the electronically excited eigenstate followed by the absorption of two more photons ionizing the atom [33, 41, 42].

At relatively lower intensities, the general features of such multiphoton ionization processes can qualitatively be understood already in a rather simple picture using the electric dipole approximation in the lowest-order perturbation theory (LOPT) [20]. "In the LOPT only the absorption of the minimum number of photons is considered that is requires to reach the final state. According to electric dipole selection rules (and neglecting electron and nuclear spins), the absorption of each photon corresponds to a $\Delta\ell = \pm 1$ and a $\Delta m = -1$, 0, or +1. Consequently, if an initial state featuring an orbital angular momentum orientation of m is ionized by the absorption of n photons, the final set of available magnetic sub-level ranges from $m - n$ to $m + n$. The final state can then be expressed in terms of a sum of the corresponding partial waves. [43].

2.2. ULTRA-COLD AND POLARIZED ATOMS

The experiments performed and analyzed within this PhD project stand out to earlier studies, because a laser cooled and polarized atomic target is used. Historically, atomic

laser cooling techniques were pioneered independently by two groups, Hänsch et al. [44], and Wineland et al. [45] in 1975 exploiting the Doppler cooling effect using near-resonant narrow bandwidth laser radiation.

This technique was enhanced making it possible to confine ultra-cold atomic samples in a small volume in magneto-optical traps (MOT) [46, 47] cooling the atoms and storing the at sub-Millikelvin temperatures for minutes or even longer. Transferring the atoms to other traps using conservative forces allows to cool them evaporatively even lower and to quantum degeneracy [48–50]. This expanded atomic physics research in ultra-cold region.

2.2.1. Magnet Optical Trap (MOT). Magneto-optical traps are powerful and widely used tools for preparing ultra-cold samples of neutral atoms. Here, atoms are cooled and trapped by using three pairs of retro-reflected laser beams overlapping in a quadrupole magnetic field forming a trapping region (see Figure. 2.3, right). In a simplified picture, the cooling and trapping of the atoms can be understood by three underlying mechanisms (a detailed explanation can be found in, e.g., [46])

The first mechanism is the spontaneous force, which allows to exert a directed force on an atom by exposing it resonant laser radiation. The atom will absorb not only the photon's energy but also its momentum, thereby receiving an impulse of $\hbar k$ (k is the photon wave number) in the laser propagation direction. The atoms will stay for some time (typ. tens of nanoseconds) in the electronically excited state, before they decay back to the ground state emitting a photon and again receiving an impulse, but this time random direction, which averages to zero. This process repeats with a rate of typically tens of Megahertz effectively resulting in a force in laser direction on the atoms.

The second mechanism is Doppler-cooling, which relies on the velocity dependent frequency shift of the laser radiation. If its frequency is slightly down-shifted from the resonance, the absorption probability is increased for atoms moving towards the laser source due to the well-known Doppler effect. Therefore, the atoms are more likely to be slowed down than to be accelerated. If atoms are subjected to laser radiation from all directions,

they will effectively be cooled. This configuration is often called "optical molasses" due to the velocity dependent nature of the force. However, it is important to note that this mechanism does not allow to confine the atoms in a trap volume.

The third mechanism is the Zeeman effect, which unfolds as a shift of atomic energy levels in an external magnetic field. Generally, the magnitude of the shift depends on the strength of the magnetic field and on the orientation of the atomic angular momentum relative to the direction of the magnetic field (i.e. it depends on the magnetic quantum number m_f). A simplified one-dimensional scheme neglecting the spins of nucleus and electrons and considering the transition between an s ground state and a p excited state is depicted in Figure. 2.3 (left). Here, only the excited state will experience a Zeeman splitting for the sub-levels with $m = -1$, 0, and +1. In the center of the trap the magnetic field is zero and the order of the sub-levels' energies reverses on both sides of the trap. Due to the detuning of the beams, the laser is in resonance slightly outside of the trapping center. If the polarization of the laser beams is chosen to be either left or right-handed circularly polarized, transitions can selectively be driven to $m = -1$ or $m = +1$, respectively, with an individual laser beam. This allows to choose a configuration, where the atoms are always pushed back towards the MOT center effectively confining the atoms in a small volume.
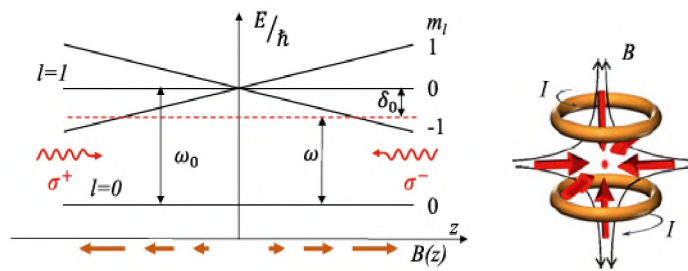
Figure 2.3. Trapping mechanism (atomic energy level scheme in MOT) (left) created by anti-Helmholtz coils(right), picture taken from [51]

The MOT is a useful tool to prepare atomic targets for different trapping and ionization experiments. However, it has limitations for its applicability to the experiments described in this thesis. How these are overcome is described in the following chapter.

2.2.2. All Optical Atom Trap (AOT). Traditional MOTs are not suited for providing a target for momentum resolved collision experiment involving polarized atoms due to two limitations: First, the position dependent direction and intensity of the magnetic field makes it essentially impossible to polarize the target atoms, because any oriented atomic magnetic moment would precede around the position dependent magnetic field axis. If the atoms are polarized at a given point in time, this precession would result in a de-polarization of the target sample after typically only hundreds of microseconds. Second, for ionization experiments it is desirable to detect electrons, reconstruct their trajectories in a spectrometer, and calculate their initial momentum. However, due to the quadrupole magnetic field, the electron trajectories depend sensitively on the starting point of the electron, which cannot directly be measured with sufficient resolution. Therefore, a momentum-resolved electron detection with high resolution is not possible out of a MOT target.

In a previous attempt to combine magneto-optical cooling and electron momentum imaging, the magnetic field was periodically switched between a quadrupole magnetic field and an homogeneous magnetic field, for the trapping of the atoms and for the detection of electrons, respectively [29] (see Figure 2.4). While this is a viable approach, it has the drawback of a reduced duty cycle, because trapping and ionization measurement can never happen simultaneously. Moreover, there are several technical challenges connected to the switching of the magnetic field, because induced voltages can be very high and slowly decaying eddy currents can alter the magnetic field from its ideal configuration.

These problems were overcome with the development of a novel all-optical trap (AOT), which was developed at Missouri S&T in 2018 [22]. In the AOT, the atoms are cooled and trapped by near-resonant laser beams in absence of the quadrupole magnetic field but only a weak homogeneous magnetic field used.
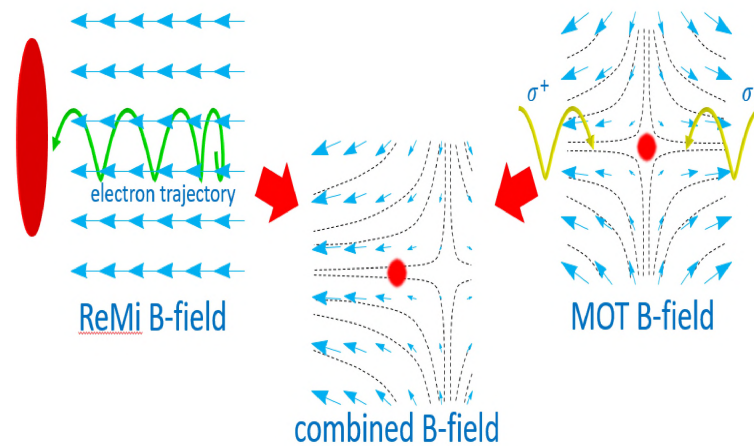
Figure 2.4. Combined B-Field (Homogeneous and quadruple magnetic fields)

Overall, this technique enables to prepare a target in a highly polarized state at very low atom temperatures and relatively high number densities up to which makes this trap ideally suited for momentum-resolved electron-ion coincidence experiments with excellent momentum resolution [25].
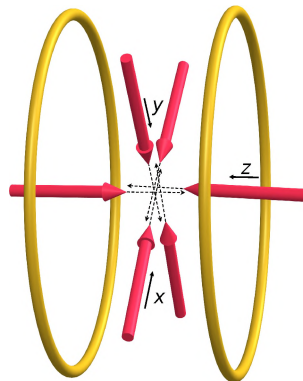
Figure 2.5. All Optical Atom Trap(AOT). Picture taken from [22]

The overall configuration of the trap is very similar to conventional magneto-optical traps. It mainly requires small modifications of laser beam geometries, polarization, and frequency which makes it easily implementable in other existing MOT experiments. A complete theoretical description of the observed trapping mechanism is still not available,

but it is believed that rectified dipole force [52–54] due to the bichromaticity [55] of the laser field is significant and might contribute to the trapping of atoms. Similar to previously reported trap configurations like "supermolasses" [56] and "Vortex trap" [57, 58], the AOT requires a proper mis-alignment from the ideal retro-reflecting configuration and the trapping efficiency is very sensitively dependent on the laser parameters. Here, the procedure to achieve stable trapping will be briefly discussed: First, the set up is started at the standard magneto-optical trap configuration, i.e., there is a quadrupole magnetic field in the trapping region and the laser beams are all circularly polarized pushing the atoms back in the trap center. Then the quadrupole field is reduced and overlaid with a homogeneous magnetic field. This will reduce the trapping efficiency which can (partially) be recovered by altering the laser position, frequency, and polarization. This process is repeated iteratively until the quadrupole field is completely turned off. At this point, the atoms are in an all-optical trap. If the polarization of all laser beams is chosen to be in the plane perpendicular to the magnetic field direction, a high degree of electronic target polarization can be achieved. Several properties of the AOT (see Figure 2.5 have been characterized and compared to conventional MOTs. The overall trapping performance of the traps can generally be described by the simple rate equation,

$$\frac{dN}{dt} = L - \Gamma N - \beta N^2 \qquad (2.4)$$

With N being the number of trapped atoms, L is the absolute loading rate, Γ is the relative linear loss rate, and β is the two-atom loss coefficient due to mutual collisions between two trapped atoms. A good trap performance and long trapping times are achieved at high loading rates L and at small loss factors Γ and β. These parameters can be measured by obtaining the loading profile starting with an empty trap ($N = 0$) and for the decay curve

staring with a full trap and switching L to zero. An example of such curves is shown in Figure 2.6. Overall, the trapped particle number as well as the trapping time for the AOT are slightly below the one of the magneto-optical trap (for details see [22]).
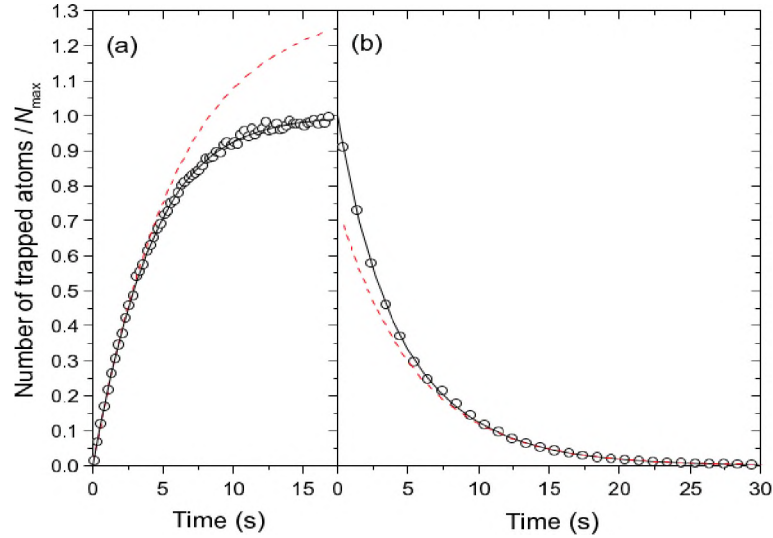
Figure 2.6. Loading (a) and decay (b) curve of the trap in AOT. Open circles show experimental data; the solid lines correspond to the fits according to Eq. 1. The dashed lines are exponential curves fitting the data for low atom number densities, where the two-atom loss term is negligible) [22]

The temperature of the atoms can be determined by measuring the ballistic expansion of the atom cloud after switching the colling lasers off for short periods. The width of cloud is determined after the switch-off by fluorescence imaging and plotted as a function of switch-off time in Figure 2.7.
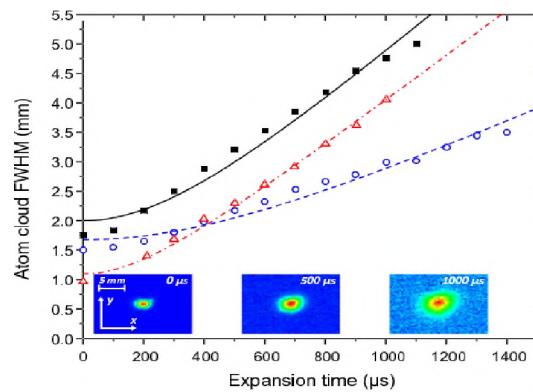
Figure 2.7. Ballistic expansion of atom cloud in AOT

Overall, number densities of $10^9/cm^3$ at temperatures of about 2 mK are achieved.Moreover, the polarization of the target cloud is estimated by measuring the polarization of the fluorescence light. About 93 % of the atoms are in a single magnetic sub-level with $m = +1$. These characteristics make the AOT ideally suited for momentum-resolved atomic ionization experiments.

2.2.3. The Optical Parametric Chirp Pulse Amplifier (OPCPA). In the experiments performed in the scope of the PhD project, lithium atoms were ionized in the intense field of a commercially available femtosecond light source. It is a Venteon OPCPA producing pulses of durations down to 8 fs at bandwidths ranging from 650 to 1000 nm. In the laser focus, intensities of up to 10^{14} W/cm^2 can be achieved.

The OPCPA consists three parts as shown in Figure. 2.8,which are an oscillator, a high power amplifier (HPA), and a non-collinear optical parametric amplifier (NOPA). The oscillator is a mode-locked Ti:Sa laser which produces broadband pulses of about 5 fs duration with a spectrum ranging from about 600 to 1200 nm. The repetition of the oscillator is with 80 MHz very high, and the power averages to about 200 mW.
The output of the oscillator cannot be directly used for ionization experiments due to the high repetition rate and the comparably low pulse energy. Therefore, a "pulse-picking" mechanism is required to reduce the repetition rate, and an amplifier has to increase the pulse energy.
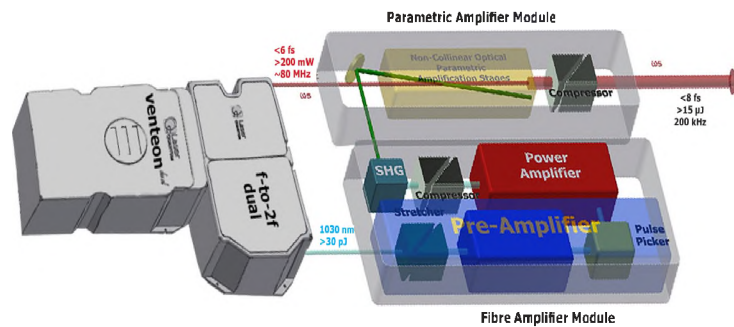
Figure 2.8. Optical parametric chirp pulse amplifier (OPCPA)

The high-power amplifier serves the task to create synchronized pump pulses at a reduced repetition rate that can be used to amplify the oscillator output. To this end, a small fraction at wavelength of 1030 nm is separated from the oscillator output, stretched in time to about 300 fs, and guided into three serial fiber amplifiers and a high power rod-type amplifier. Pulse pickers are reducing the repetition rate to 200 kHz. After the amplifier rod, the pulse is compressed by grating compressor to a duration of 150 fs with an average power of 48 W. These pulses are then focus into a nonlinear crystal to produce second harmonic generation at 515 nm with a power of $20W$.

The final output of the OPCPA is created in two serial NOPA stages [59, 60]. Generally, a NOPA stage consist a nonlinear crystal where energy is transferred from a pump beam to a seed beam which both are overlapped in the crystal. In our setup, the seed beam is the main broadband output of the oscillator, while the pump beam corresponds to the output of the HPA. After the two NOPA stages, an average power of up to 2 W at a repetition rate of 200 kHz and pulse durations down to 8 fs can be achieved.

It is important to note that the operation of the NOPA stages can be modified either creation broad bandwidth pulses with very short duration or pulses that are longer in time but feature a narrower spectrum with tunable center wavelength. The latter mode of operation was extensively used throughout the projects reported here.

2.2.4. Cold Target Recoil Ion Momentum Spectroscopy (COLTRIMS). It is an imaging technique to obtain on the fragmentation dynamics of a few body system by measuring the outgoing particles' momentum vectors [23, 24]. In brief, all charged fragments from an atomic, molecular reaction are projected by a combination of electric and magnetic fields on position sensitive detectors. Knowing the charge and mass of the particles, their starting point, and the field configuration, the momentum vectors can be calculated for the measured time-of-flight and the position on the detector.

In the experiments performed for this PhD project, the field configuration was particularly simple: Both fields, electric and magnetic, were homogeneous and in z-direction. The motion of charged particle is obtained in non-relativistic approximation by the Lorentz Force Law. The force on a particle of charge q and mass m traveling in the static electric and magnetic fields $\vec{E}(\vec{r})$ and $\vec{B}(\vec{r})$, respectively, is given by

$$\vec{F}(\vec{r}, \vec{v}) = \frac{m\mathrm{d}^2\vec{r}}{\mathrm{d}t^2} = q(\vec{E}(\vec{r}) + \vec{v} \times \vec{B}(\vec{r})) \tag{2.5}$$

For both fields pointing in z-direction[51], this differential equation has the solution

$$x(t) = \frac{1}{qB_z}\left(\sin(\omega_c t)p_{0x} + (1 - \cos\omega_c t)p_{0y}\right) \tag{2.6}$$

$$y(t) = \frac{1}{qB_z}\left(\sin(\omega_c t)p_{0y} + (\cos\omega_c t - 1)p_{0x}\right) \tag{2.7}$$

$$z(t) = \frac{p_{0z}}{m}t + \frac{qE_z}{2m}t^2 \tag{2.8}$$

For a particle starting with the initial momentum components p_{0x}, p_{0y}, and p_{0z} at the origin. Here $\omega_c = qB_z/m$ is the cyclotron frequency of the particle.

If the particle hits the detector after time T at the (three-dimensional) position $x(T) = x_d$, $y(T) = y_d$, and $z(T) = z_d$, the starting momentum of the particle can be calculated from the above equations to be

$$p_{0x} = \frac{qB_z}{2}\left(\frac{\sin\omega_c T}{1 - \cos\omega_c T}x_d - y_d\right) \tag{2.9}$$

$$p_{0y} = \frac{qB_z}{2}\left(\frac{\sin(\omega_c T)}{1 - \cos\omega_c T}y_d + x_d\right) \tag{2.10}$$

$$p_{0z} = \frac{z_d m}{T} - \frac{qE_z}{2}T \tag{2.11}$$

The achievable momentum resolution depends on the uncertainty of the positions and the time-of-flights, which in term depend on the size of the reaction volume as well as the initial temperature of the target. Due to extremely low target temperatures and a very small laser focus, an final resolution of only about 0.01 a.u. for the electrons and about 0.03 a.u. for the recoil ions was achieved.

PAPER

I. MAGNETIC DICHROISM IN THE FEW-PHOTON IONIZATION OF POLARIZED ATOMS

B.P. Acharya[1], M.Dodson[2], S.Dubey[1], K.L.Romans[1], A.H.N.C.DeSilva[1], K.Foster[1], O.Russ[1], K.Bartschat[3], N.Douguet[2], and D.Fischer[1]

[1]Department of Physics Missouri University of Science and Technology
Rolla, Missouri 65409

[2]Department of Physics, Kennesaw State University
Kennesaw, Georgia 30144, USA

[3]Department of Physics and Astronomy, Drake University
Des Moines, Iowa 50311, USA

ABSTRACT

We investigate few-photon ionization of an atomic target with linearly polarized light and demonstrate that angular asymmetries can occur provided the target atom is initially polarized. Specifically, lithium atoms are prepared in an all-optical laser atom trap (AOT), excited to the polarized Li($2p$, m=+1) state, and ionized by interacting with femtosecond laser pulses. Shifts of the main electron emission angles away from the laser electric field axis are observed, which vary with laser intensity and wavelength. The experimental spectra are in very good agreement with the results of our theoretical model based on the numerical solution of the time-dependent Schrödinger equation (TDSE). Qualitatively, the observations are explained in a perturbative picture using the electric dipole approximation. Here, angular asymmetries are traced back to interferences of partial waves with two or

more contributing angular momenta ℓ and a non-vanishing mean angular momentum $\langle m \rangle$ in the final state. This allows to obtain complete quantum mechanical information of the electronic final state including its complex phase.

1. INTRODUCTION

Atomic ionization in optical fields proceeds predominantly through the electric dipole interaction of the initially bound atomic system with the external field. Consequently, photoelectron angular distributions (PAD) are generally governed by the direction and symmetries of the electric field. In the simplest case of an unpolarized target, which is ionized by linearly (or circularly) polarized light, the symmetries of the electronic final state are (in the electric dipole approximation) identical to the symmetries of the ionizing field given by its Stokes parameters. However, there are more complex situations where these symmetries are lifted and the electron emission does not geometrically align with the dominant electric field direction.

Examples, which have been debated extensively in the past decade, are 'attoclock' experiments [3, 7, 19, 25, 27] where adiabatic tunnel ionization of atoms in carrier-envelope phase stabilized elliptically polarized few-cycle pulses is investigated. In these measurements, the electron angular distributions feature a shift from the direction of the strongest electric field in the plane perpendicular to the laser propagation direction (i.e. in the *azimuthal* plane). This shift in the azimuthal angle φ is (partially) attributed to a time delay of the ionization while the electron tunnels through the barrier formed by the potential of the atomic core and the adiabatically changing electric field of the laser. While this interpretation is not uncontroversial and the debate about the tunneling time in strong field physics is still open (for recent reviews, see [17, 28]), the joint experimental and theoretical efforts resulted in a much better understanding of the tunneling dynamics and an improved modeling of the complex strong-field atom interaction.

Already two decades before the first attoclock experiments, a related phenomenon has been observed in the multi-photon ionization regime – the so-called "elliptic dichroism" [2]. Here again, the major and minor axes of the polarization ellipse do not represent lines of reflection symmetry in PADs measured in noble gas ionization by elliptically polarized light. While the observed symmetry breaks are in contradiction to Keldysh-type theories [2, 8, 16, 26], they are qualitatively explained in terms of the lowest-order perturbation theory (LOPT) [18, 22]. In this description, the asymmetry in the azimuthal electron emission angle φ is a result of the interference of phase-shifted partial waves with different orbital angular momentum quantum numbers ℓ and m_ℓ.

In the following decades, elliptic dichroism attracted considerable interest and it was observed, for instance, in above threshold ionization of rare gas targets [23, 24] as well as in few-photon ionization of alkali atoms [35]. In contrast to the ionization by purely linearly or circularly polarized light, analyzing ionization data for elliptic polarization enables to extract phases and amplitudes of the final partial waves, thereby allowing to obtain the *complete* quantum mechanical information of the scattering process [6, 34]. Recently, it was predicted that a maximum elliptic dichroism can be achieved in two-photon ionization for an appropriate choice of the wavelength of the radiation making it a promising tool, e.g., to analyze the polarization state of free electron laser radiation [13]. It is worth noting that the ellipticity of the polarization is not a *sine qua non* for angular asymmetries to occur. Similar asymmetric final states are expected, e.g., in the multi-photon ionization by two combined laser beams of different color, one with linear and the other one with circular polarization [32].

In the present study, we demonstrate that left-right asymmetries can already be achieved in the atomic ionization by purely linearly polarized light, if the target atoms are initially polarized. On the experimental side, it has been shown previously that optical traps are an ideal tool to provide excited and polarized atomic targets for ion-atom scattering [14, 20] or photoionization experiments [4, 33, 36]. Here, we use an all-optical atom trap

(AOT) [30] to prepare an excited lithium target in the polarized Li($2p$, $m = +1$) state. The atoms are ionized in femtosecond laser pulses with a wavelength varied between about 695 nm and 800 nm. We observe strong *magnetic* dichroism, i.e. a dependence of the differential cross sections on the magnetic quantum number of the initial state [21], which manifests itself in angular shifts of the main electron emission directions with respect to the laser polarization axis. The measured spectra are well reproduced by our model based on the numerical solution of the time-dependent Schrödinger equation (TDSE), and strongly depend on both the intensity and wavelength of the laser pulse.

The observed asymmetries are qualitatively explained in a perturbative picture in terms of the LOPT in the electric dipole approximation analogous to the discussions in [13, 18, 22]. Despite its similarities to elliptical dichroism, the present scheme does not require non-linear interactions with the laser field in order for asymmetries to appear [13], but they are, in principle, present already after the absorption of only a single photon [33]. Moreover, the present approach can, in future, contribute to the ongoing discussion about tunneling times in attoclock experiments, because it possibly allows to disentangle contributions to the angular shifts caused by the tunneling dynamics and by other effects such as, e.g., the long-range Coulomb interaction between the emitted electron and the target core.

2. EXPERIMENT

The experimental setup has been described previously [4, 31, 33], so only a brief summary is given here. It consists of three major components: First, an optical trap providing state-prepared lithium target atoms; Second, a tunable femtosecond laser source generating the ionizing external field; And third, a "Reaction Microscope" measuring the momentum vectors of the ionization products.

The lithium target cloud is prepared in a near-resonant all-optical laser atom trap (AOT) [30], where the atoms are cooled to temperatures in the milli-Kelvin range and confined to a small volume of about 1 mm diameter. The cooling laser system consists of an external cavity diode laser with a tapered amplifier, whose frequency is stabilized near the ^{6}Li D2-transition at about λ= 671 nm. The radiation couples the $2S_{1/2}$ to the $2P_{3/2}$ state, and – in steady state – about 25 % of the target atoms populate the excited p level with about 93 % of them being in a single magnetic sub-state with $m_\ell = +1$ with respect to the direction of a weak magnetic field (the z-direction).

The femtosecond laser source is a commercially available system based on a Ti:Sa oscillator with two non-collinear optical parametric amplifier (NOPA) stages (e.g. [12]) providing maximum pulse energies of up to 15 μJ at a repetition rate of 200 kHz. The system can be operated in a short-pulse (about 7 fs) broadband mode (ca. 660nm-1000nm). However, in the present experiment we amplified only a rather narrow bandwidth ($\pm$15 nm) resulting in pulse durations of about 35 fs. The laser beam is guided into the vacuum chamber and focused into the lithium cloud with a minimum beam waist of about 50 μm.

A cold target recoil ion momentum spectrometer (COLTRIMS) – also referred to as "Reaction Microscope" [9, 15] – is employed to measure the three-dimensional momentum vectors of electrons and recoil ions after the ionization process. The differential cross section of the ionization of the Li(2s) ground state and of the Li(2p, $m_\ell = +1$) excited state are extracted following a switching procedure that is described in more detail in [31]. A typical electron momentum resolution of 0.005 to 0.01 a.u. is achieved [33].

3. THEORY

The experimental data is compared to *ab initio* calculations based on solving the time-dependent Schrödinger equation (TDSE) considering a single-active electron (SAE) in a He-like $1s^2$ ionic core. A static Hartree potential [1, 29] is used and supplemented by phenomenological terms, which are discussed in [4]. As shown earlier [31], our model

potential describes the atomic structure with an accuracy of better than 1 meV for the $n = 2$ and $n = 3$ states. Previous calculations using the same code yield excellent agreement with experimental data measured under similar conditions [4].

4. RESULTS AND DISCUSSION

In Figure. 1, the momentum and angular distributions for the ionization of the initial $2s$ and $2p$ states are shown for a center wavelength of 770 nm and a peak intensity of $1.8 \cdot 10^{11}$ W/cm^2. The laser field is polarized along the y axis, and the orbital angular momentum of the excited p state is polarized in the z direction perpendicular to the drawing plane. For all data presented in this study, the given laser field parameters resulted in Keldysh parameters well above 10. Therefore, the ionization process can be described in the multi-photon picture. The initial s state is ionized by the absorption of four photons resulting in a final state momentum of about 0.28 a.u., reflected in a single ring structure in the momentum distribution (see Figure. 1). The p state ionization proceeds through the absorption of three photons corresponding to a slightly larger final state momentum of about 0.31 a.u.. For the ground state ionization, the angular differential cross section is symmetric with respect to the laser polarization axis (the y axis in the graph) with its highest intensity in the direction of the laser electric field at $\varphi = 90°$ and 270°. Notably, this symmetry is broken for the p state ionization and the peaks in the angular distribution are shifted away from the electric field direction by about 10°.

For a rigorous comparison of the measured spectra with the calculations, the non-uniform spatial intensity distribution of the laser field around the focal point needs to be considered. In the experiment, the location of a specific ionization event is not precisely known and, therefore, our experimental data is not measured for a well-defined intensity, but averaged over an intensity range. In previous studies, we have convoluted the theoretical cross sections over a broad intensity range (e.g., [4]), which yielded nearly perfect agreement between measurement and calculation. In the present case, we omitted this
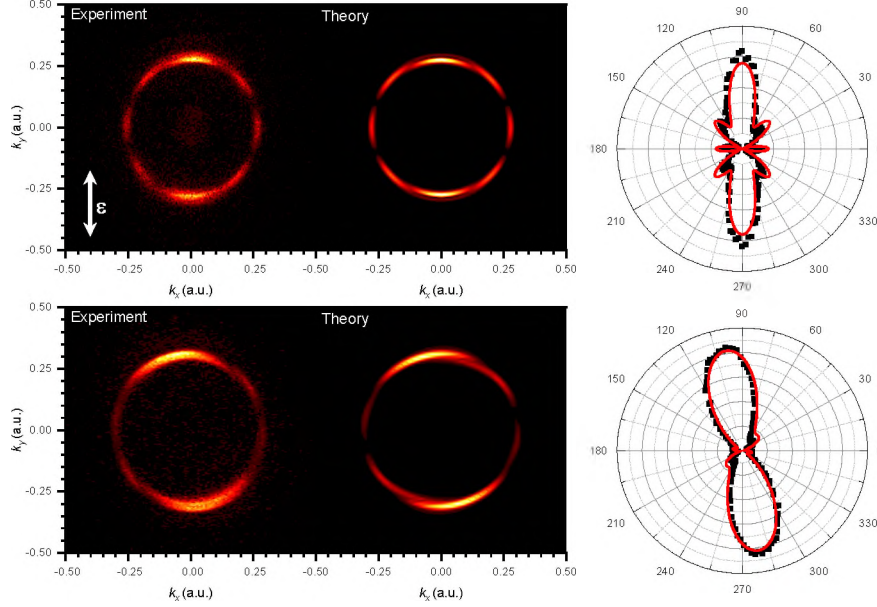
Figure 1. Differential cross sections for few photon ionization of lithium atoms initially in the 2s (top) and 2p(m=+1) (bottom) state in 35 fs laser pulses at a center wavelength of 770 nm and a peak intensity of $1.8 \cdot 10^{11}$ W/cm^2.] The initial 2p state is polarized along the z direction (perpendicular to the drawing plane), the laser field is polarized in the y direction (i.e. vertically). Left and center column show experimental and theoretical momentum distributions, respectively. The right column shows the distribution of the azimuthal angle. All spectra represent cuts in the xy-plane, i.e. z = 0.

convolution. While we expect that this procedure would reduce discrepancies, intensity dependent features of the calculated spectra are more clearly visible without the averaging. Instead, we performed the calculation for a mean intensity which is by a factor of 1.8 lower than the peak intensity applied in the experiment. Overall, the shape of the measured and calculated spectra are in excellent agreement (see Figure. 1).

The general features observed in the photoelectron angular distributions can qualitatively be explained in a picture based on the lowest order perturbation theory (LOPT). In the electric dipole approximation, the selection rules yield a change of the magnetic quantum number m (with respect to the laser propagation direction) by +1 or −1 for right and left-handed circularly polarized light, respectively. Because the linearly polarized radiation used in our experiment corresponds to the coherent superposition of the two circular polar-
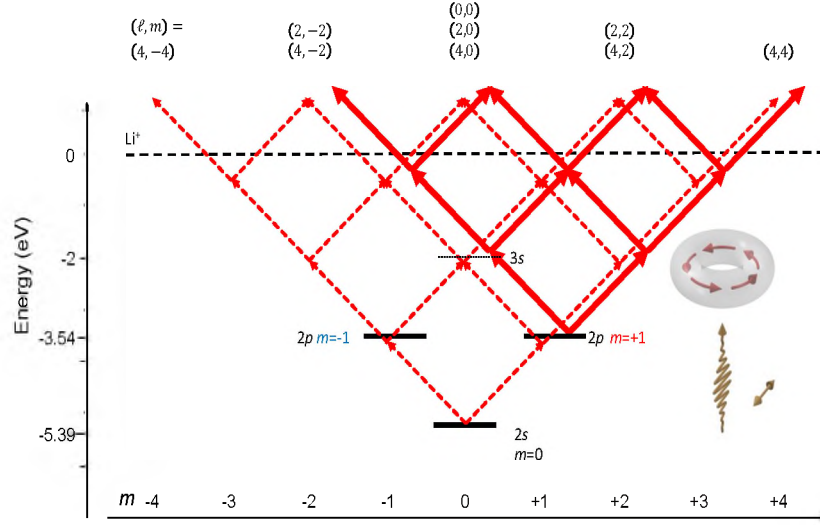
Figure 2. Ionization scheme for three-photon ionization of the $2p$ excited state (solid arrows) as well as for four-photon ionization of the $2s$ ground state (dashed arrows) in a field with linear polarization oriented perpendicular to the atomic quantization direction.

izations, the magnetic quantum number is changed simultaneously by $+1$ and -1 for each absorbed photon. The resulting ionization pathways are depicted in Figure. 1. The angular part of the final electronic continuum state can be expressed in terms of a superposition of spherical harmonics $Y_{\ell m}(\vartheta, \varphi)$ of different dipole-allowed quantum numbers ℓ and m, which are $\ell = 0$, 2, and 4 (corresponding to s, d, and g waves) and $m = -2, 0, 2$, and 4 in the presently considered case of 3-photon ionization of a $2p\,(m = +1)$ initial state.

Considering only the dependence on the azimuthal angle φ (e.g. for $\vartheta = 90°$), the differential cross section can be written as (see e.g. [22])

$$\frac{d\sigma}{d\Omega} = \left| \sum_{\ell,m} a_{\ell m} e^{im\varphi} \right|^2 \tag{1}$$

with $a_{\ell m}$ relating to the complex amplitudes of the contributing partial waves. It is important to note that the phases of the amplitudes depend on the orbital angular momentum ℓ, because the radial part of the outgoing electron wave has an asymptotic form of $\exp(ikr + i/k \ln r + i\delta_\ell)$

featuring the phase shift δ_ℓ due to the interaction of the outgoing electron with target core, which includes generally both Coulombic and non-Coulombic contributions. Performing the summation over ℓ, the above equation simplifies to

$$\frac{d\sigma}{d\Omega} = \left| \sum_m c_m e^{im\varphi} \right|^2 \tag{2}$$

with $c_m = \sum_\ell a_{\ell m}$ being complex. Any φ-dependence of the cross section is a result of the interference of partial waves with different m.

For the specific case shown in Figures. 1 the quantum number m can take four values $(-2, 0, 2, \text{and } 4)$. In this case, the differential cross section of Eq. 2 can be written in the form

$$\begin{aligned} \frac{d\sigma}{d\Omega} &= A + B \cdot \cos(2\varphi + \Delta_2) + C \cdot \cos(4\varphi + \Delta_4) + \\ &\quad D \cdot \cos(6\varphi + \Delta_6) \end{aligned} \tag{3}$$

with real factors A, B, C, and D. The first term in this equation represents the sum of the absolute squares of the partial wave amplitudes, i.e. $A = \sum |c_m|^2$. The second, third, and fourth terms relate to the interferences between pairs of partial waves whose m differs by 2, 4, and 6, respectively. Generally, the expression in Eq. 2 corresponds to an angular distribution with six local maxima in accordance with our data shown in Figure. 1 (bottom). The lifting of mirror symmetry observed in the data stems from the angular shifts Δ_2, Δ_4, and Δ_6. It is straight-forward to show, that (at least) two conditions need to be fulfilled for the angular shifts not to vanish: (i) The final state needs to feature an asymmetric m distribution, i.e. there is a non-zero mean polarization with $\langle m \rangle \neq 0$. And (ii), there must be an additional non-vanishing phase difference between interfering partial waves (apart of the trivial φ-dependent phase). The first requirement is generally fulfilled for a polarized

target in an initial state with $m \neq 0$, or if the target is ionized by elliptically polarized light. The latter condition is satisfied if different angular momenta ℓ contribute to the final state due to the phase shift of the radial part of the wave function.

According to the perturbative picture discussed above, the angular shifts observed in the data are sensitive not only to the relative magnitude of the partial wave amplitudes, but especially to their relative phases. These phases stem from the complex angles δ_ℓ of the outgoing (radial) wave functions, which are different for each ℓ. Neglecting the dressing of the atom in the laser field, the phase angles δ_ℓ depend only on the continuum energy of the electron and on the target core potential, but not on the detailed parameters of the laser field and on the atomic structure. Therefore, the shifts observed in the angular distributions are expected to change with the electron continuum energy and, hence, with the laser wavelength. However, a change of the angles can also be anticipated for varying laser intensities, because they influence the relative magnitudes of final state partial wave amplitudes. In order to get a more complete picture of these dependences, we have studied the angular distributions for a range of laser parameters (see Figure. 3). In the figure, the spectra for the ionization of the $2s$ and $2p$ states are cross-normalized and, when indicated, multiplied with a given factor for a better visibility.

Overall, the shape of the angular distributions agrees very well between measured and calculated data with some moderate discrepancies at 770 nm and 800 nm. The relative magnitudes of the $2s$ and $2p$ ionization cross sections vary vastly over the investigated wavelength and intensity regime. Also here, some discrepancies are observed, which are largest for 770 nm at $3 \cdot 10^{11} \, \mathrm{W/cm^2}$ (with a factor of about 2). As mentioned above, an averaging of our theoretical spectra over the experimental intensity distribution is expected to improve the agreement. However, we opted for not doing that in the present study, because intensity dependent changes of the cross sections are more clear without this convolution. Moreover, we have shown earlier [4, 31] that our theoretical model describes the target system very accurately and the numerical uncertainty is extremely small. Remaining dif-

ferences could still stem from experimental uncertainties in the laser parameters (e.g. pulse duration, spectrum, and intensity) which are very challenging to characterize accurately. Therefore, our primary aim is not the rigorous test of our theoretical model, but rather a better understanding of few-photon ionization dynamics and the mechanisms at play.

All the angular distributions shown in Figure. 3 feature two main peaks in opposite directions, which align with the laser polarization axis for the ionization of the $2s$ ground state and are shifted from this axis for the ionization of the polarized $2p$ state. This angular shifts are towards smaller angles for the wavelengths of 695 nm and 735 nm. For 770 nm, the shifts are reversed in the experimental spectra. In the calculation in contrast, the direction of the shifts seems to flip with the intensity. For 800 nm, the peaks align closely with the laser polarization axis, with the calculation showing a small shift towards smaller angles for the higher intensity.

As discussed above, the angular shifts depend sensitively on the relative magnitudes of the final state partial wave amplitudes. Atomic resonances can affect these magnitudes significantly. The most notable 1-photon resonance close to the investigated wavelength range is the $2p$–$3s$ resonance at a wavelength of 812 nm. Because the $3s$ state is spherically symmetric, all flux proceeding through this resonance will loose any information on the initial polarization direction. Therefore, this resonance can be expected to reduce the angular asymmetry. Indeed, the angular shift for a laser wavelength of 800 nm (Figure. 3, bottom) is barely noticeable. There are many 2-photon resonances between the $2p$ state and higher lying states, e.g. with $n = 6, 7, 8$, and 9 at wavelengths of about 780 nm, 760 nm, 744 nm, and 735 nm, respectively. Here, only p and f states couple to the initial $2p$ state due to dipole selection rules. It is difficult to pin the effects of these resonances down for specific laser parameters. Generally, if p-state is transiently populated after the absorption of two photons, the m quantum numbers finally populated range only from -2 to 2 and the contribution of $m = 4$ is suppressed. This reduces effectively the contribution of the last

term in Eq. 2, which is responsible for the six peak structure. A resonance to an f state, in contrast, will allow for all even m quantum numbers between -2 and 4 in the final state.
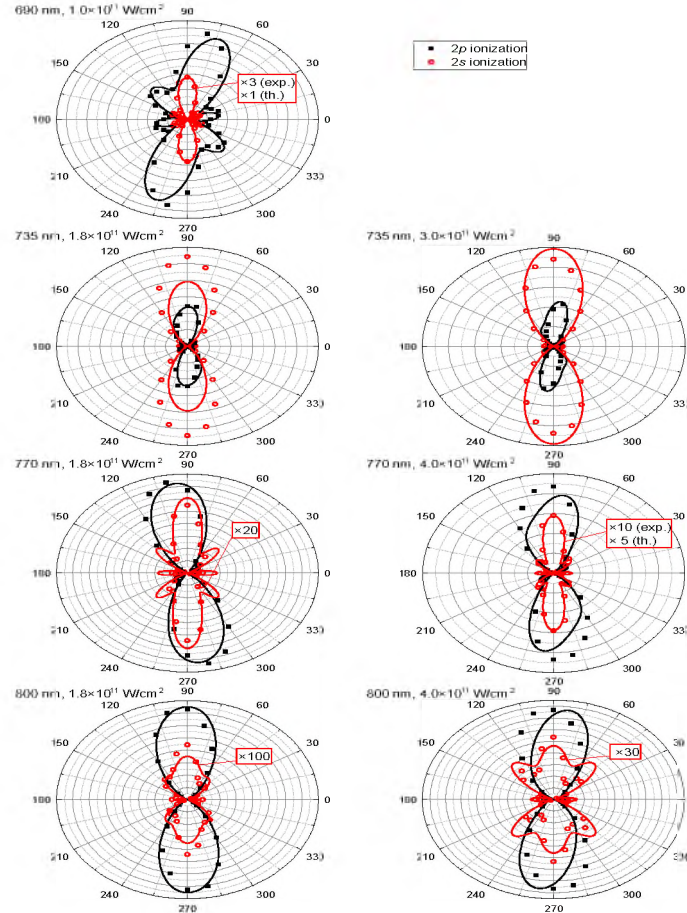
Figure 3. Same as Figure. 1(right), but for different laser wavelengths and intensities, which are denoted at each graph individually. Black solid squares and black lines correspond to experimental and theoretical results for the initial $2p$ state, respectively. Red open circles and red lines represent the according data for the initial $2s$ state. The data for the two initial states are cross-normalized in each graph, and – where indicated – multiplied by the given factor for better visibility.

The shortest wavelength studied is 695 nm and it stands out in several respects: First and foremost, the absorption of only two photons suffices to promote the $2p$ electron to the continuum at this wavelength. The final electron energy is just above threshold and the main intensity of both $2s$ and $2p$ ionization cross sections is at very small momenta well below 0.1 a.u. (see Figure. 4). Furthermore, there is no significant resonance-enhancement at this

wavelength, which makes this system a particularly clean manifestation of the observed dichroic asymmetries. Indeed, the observed angular shift of the two dominant peaks is with about 15° stronger than in all other cases investigated. The calculations reproduce the momentum distributions observed experimentally with excellent agreement.
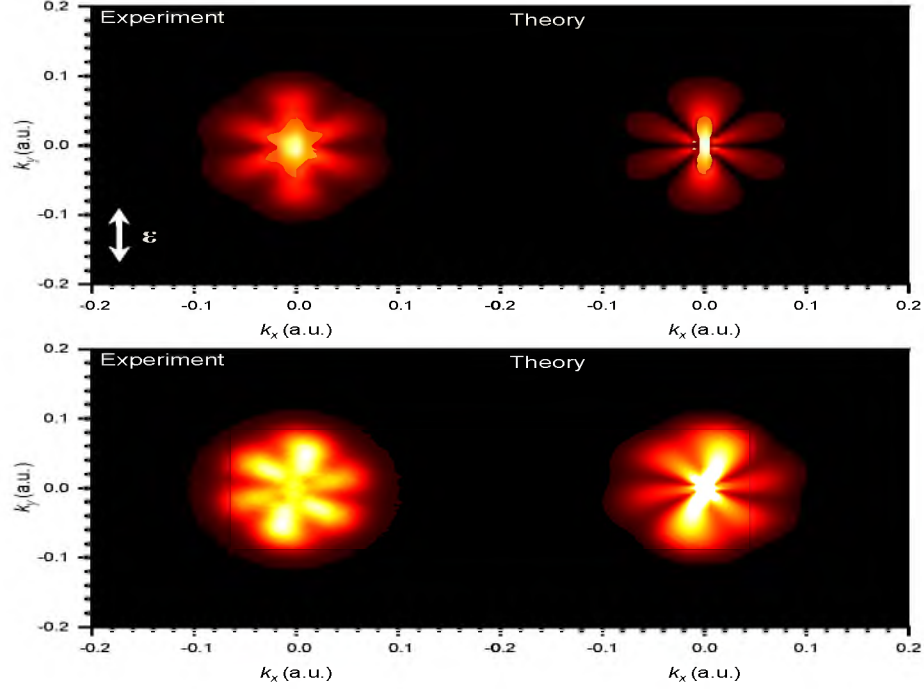
Figure 4. Same as Figure. 1 (left and center), but for a laser wavelength of 695 nm at a peak intensity of $1 \cdot 10^{11}$ W/cm^2.

The lower number of absorbed photons gives rise to different angular momenta contributing to the final state. Here a superposition of p and f waves with magnetic quantum numbers $m = -1, 1$, and 3 are expected in the LOPT. This results in a vanishing of the last term in the angular differential cross section of Eq. 2 and only 4 peaks are expected. However, this is in direct contradiction to our measured and calculated spectra where six peaks can clearly be identified. While this evident violation of the LOPT at the present comparably low intensities might be surprising, it can be explained by a peculiarity of the investigated system: The present laser wavelength is close to the $2s$–$2p$ resonance at 671 nm, and the laser field couples the polarized initial state to the ground state. Therefore,

a fraction of the flux is passing through the atomic ground state giving rise to a contribution of $m = -3$ to the final state, which is not considered in LOPT and results in the observed six peak structure.

5. SUMMARY AND CONCLUSION

We investigated magnetic dichroism in differential cross sections of atomic few-photon ionization of polarized atoms by linearly polarized femtosecond optical laser pulses. Here, dichroic asymmetries manifest itself in the photoelectron angular distributions as a lifting of reflection symmetry with respect to the laser polarization axis, and an angular shift of the main electron emission directions away for the electric field orientation is observed. Very Similar asymmetries have been reported earlier for rather different reactions, e.g., for electron [5] or ion [10, 11, 14] impact ionization of polarized atoms. However, compared to these earlier studies the present systems are particularly fundamental, because of the well-defined energy and limited angular momentum transfer in the multiphoton absorption process. We studied the dependence of the angular shift on laser wavelength and intensity, and obtained very good agreement between our experimental data and an *ab initio* calculation based on the numerical solution of the time dependent Schrödinger equation.

The observed asymmetries are qualitatively discussed in a simple picture based on the electric dipole approximation in the lowest order perturbation theory. Here, the final state is expressed as a superposition of partial waves of different orbital angular momenta ℓ with orientations m. Depending on the number of photons absorbed, the quantum numbers ℓ and m are either all even or all odd. For an asymmetry to occur, two conditions have to be fulfilled: First, the final state has to feature a non-vanishing mean angular momentum, i.e. $\langle m \rangle \neq 0$. Second, at least two different angular momenta ℓ have to contribute to the final state, because they introduce complex phase differences between partial waves.

In the presently studied systems, both above mentioned conditions are met. Here, the final polarization of the electron angular momentum is essentially a "remnant" of the initial target polarization, which is (partially) preserved through the ionization process. Furthermore, several final ℓ quantum numbers are dipole-allowed in the present systems, resulting in non-zero phase angles between contributing partial waves and, eventually, in the observed angular shifts. In principle, the direct connection between photoelectron angular distributions and complex phase shifts enables to extract phase information about the final state from the data [33], which is not easily possible in conventional multiphoton experiments with unpolarized targets. It should be mentioned that the qualitative explanation given here is consistent with previous analyzes of elliptic dichroism in multiphoton ionization of unpolarized atoms [18, 22] where the mean polarization $\langle m \rangle$ of the final electron state stems from an asymmetric transfer of angular momentum by the elliptically polarized photon field.

The general methods presented here might help to answer related questions about light-matter interaction that are presently under investigation. In 'Attoclock' experiments, e.g., angular asymmetries are observed in the tunnel ionization regime in elliptically polarized carrier-envelope phase stabilized few-cycle pulses and interpreted in terms of a finite time-delay of the tunneling process [7, 25]. Future experiments involving polarized targets at much smaller Keldysh parameters than in the present study may shed light on open questions about the role of tunneling time delays and of phase shifts due to the target potential thereby improving our understanding of the fundamentally important quantum mechanical tunneling process.

ACKNOWLEDGMENTS

REFERENCES

[1] Albright, B. J., Bartschat, K., and Flicek, P. R., 'Core potentials for quasi-one-electron systems,' Journal of Physics B: Atomic, Molecular and Optical Physics, 1993, **26**(3), pp. 337–344, doi:10.1088/0953-4075/26/3/008.

[2] Bashkansky, M., Bucksbaum, P. H., and Schumacher, D. W., 'Asymmetries in above-threshold ionization,' Physical Review Letters, 1988, **60**(24), pp. 2458–2461, doi: 10.1103/physrevlett.60.2458.

[3] Camus, N., Yakaboylu, E., Fechner, L., Klaiber, M., Laux, M., Mi, Y., Hatsagortsyan, K. Z., Pfeifer, T., Keitel, C. H., and Moshammer, R., 'Experimental evidence for quantum tunneling time,' Physical Review Letters, 2017, **119**(2), p. 023201, doi: 10.1103/physrevlett.119.023201.

[4] De Silva, A. H. N. C., Moon, T., Romans, K. L., Acharya, B. P., Dubey, S., Foster, K., Russ, O., Rischbieter, C., Douguet, N., Bartschat, K., and Fischer, D., 'Circular dichroism in atomic resonance-enhanced few-photon ionization,' Phys. Rev. A, 2021, **103**, p. 053125, doi:10.1103/PhysRevA.103.053125.

[5] Dorn, A., Elliott, A., Lower, J., Weigold, E., Berakdar, J., Engelns, A., and Klar, H., 'Orientational dichroism in the electron-impact ionization of laser-oriented atomic sodium,' Phys. Rev. Lett., 1998, **80**, pp. 257–260, doi:10.1103/PhysRevLett.80.257.

[6] Dulieu, F., Blondel, C., and Delsart, C., 'Multiphoton angular distributions with elliptically polarized light. i. analytic ellipticity dependence of photoelectron distributions in the polarization plane,' Journal of Physics B: Atomic, Molecular and Optical Physics, 1995, **28**(17), pp. 3845–3859, doi:10.1088/0953-4075/28/17/021.

[7] Eckle, P., Pfeiffer, A. N., Cirelli, C., Staudte, A., Dorner, R., Muller, H. G., Buttiker, M., and Keller, U., 'Attosecond ionization and tunneling delay time measurements in helium,' Science, 2008, **322**(5907), pp. 1525–1529, doi:10.1126/science.1163439.

[8] Faisal, F. H. M., 'Multiple absorption of laser photons by atoms,' Journal of Physics B: Atomic and Molecular Physics, 1973, **6**(4), pp. L89–L92, doi:10.1088/0022-3700/6/4/011.

[9] Fischer, D., 'Recoil ion momentum spectroscopy with laser-cooled targets,' 2019, pp. 103–156, doi:10.1515/9783110580297-006.

[10] Ghanbari-Adivi, E., Fischer, D., Ferreira, N., Goullon, J., Hubele, R., LaForge, A., Schulz, M., and Madison, D., 'Comparison of experimental and theoretical fully differential cross sections for single ionization of the $2s$ and $2p$ states of li ions,' Phys. Rev. A, 2016, **94**, p. 022715, doi:10.1103/PhysRevA.94.022715.

[11] Ghanbari-Adivi, E., Fischer, D., Ferreira, N., Goullon, J., Hubele, R., LaForge, A., Schulz, M., and Madison, D., 'Comparison of experimental and theoretical fully differential cross sections for single ionization of the $2s$ and $2p$ states of li by li2 ions,' Journal of Physics B: Atomic, Molecular and Optical Physics, 2017, **50**(21), p. 215202, doi:10.1088/1361-6455/aa8dd2.

[12] Harth, A., Guo, C., Cheng, Y.-C., Losquin, A., Miranda, M., Mikaelsson, S., Heyl, C. M., Prochnow, O., Ahrens, J., Morgner, U., L'Huillier, A., and Arnold, C. L., 'Compact 200 kHz HHG source driven by a few-cycle OPCPA,' Journal of Optics, 2017, **20**(1), p. 014007, doi:10.1088/2040-8986/aa9b04.

[13] Hofbrucker, J., Volotka, A., and Fritzsche, S., 'Maximum elliptical dichroism in atomic two-photon ionization,' Physical Review Letters, 2018, **121**(5), doi: 10.1103/physrevlett.121.053401.

[14] Hubele, R., Schuricke, M., Goullon, J., Lindenblatt, H., Ferreira, N., Laforge, A., Brühl, E., de Jesus, V. L. B., Globig, D., Kelkar, A., Misra, D., Schneider, K., Schulz, M., Sell, M., Song, Z., Wang, X., Zhang, S., and Fischer, D., 'Electron and recoil ion momentum imaging with a magneto-optically trapped target,' Review of Scientific Instruments, 2015, **86**(3), p. 033105, doi:10.1063/1.4914040.

[15] Hubele, R., Schuricke, M., Goullon, J., Lindenblatt, H., Ferreira, N., Laforge, A., Brühl, E., de Jesus, V. L. B., Globig, D., Kelkar, A., Misra, D., Schneider, K., Schulz, M., Sell, M., Song, Z., Wang, X., Zhang, S., and Fischer, D., 'Electron and recoil ion momentum imaging with a magneto-optically trapped target,' Review of Scientific Instruments, 2015, **86**(3), p. 033105, doi:10.1063/1.4914040.

[16] Keldysh, L., 'Ionization in the field of a strong electromagnetic wave,' JETP, 1965, **20**(5), p. 1307.

[17] Kheifets, A. S., 'The attoclock and the tunneling time debate,' Journal of Physics B: Atomic, Molecular and Optical Physics, 2020, **53**(7), p. 072001, doi:10.1088/1361-6455/ab6b3b.

[18] Lambropoulos, P. and Tang, X., 'Comment on "asymmetries in above-threshold ionization",' Physical Review Letters, 1988, **61**(21), pp. 2506–2506, doi: 10.1103/physrevlett.61.2506.

[19] Landsman, A. S., Weger, M., Maurer, J., Boge, R., Ludwig, A., Heuser, S., Cirelli, C., Gallmann, L., and Keller, U., 'Ultrafast resolution of tunneling delay time,' Optica, 2014, **1**(5), p. 343, doi:10.1364/optica.1.000343.

[20] Leredde, A., Fléchard, X., Cassimi, A., Hennecart, D., and Pons, B., 'High-resolution probe of coherence in low-energy charge exchange collisions with oriented targets,' Physical Review Letters, 2013, **111**(13), p. 133201, doi: 10.1103/physrevlett.111.133201.

[21] Meyer, M., Grum-Grzhimailo, A. N., Cubaynes, D., Felfli, Z., Heinecke, E., Manson, S. T., and Zimmermann, P., 'Magnetic dichroism in k-shell photoemission from laser excited li atoms,' Phys. Rev. Lett., 2011, **107**, p. 213001, doi: 10.1103/PhysRevLett.107.213001.

[22] Muller, H. G., Petite, G., and Agostini, P., 'Comment on "asymmetries in above-threshold ionization",' Physical Review Letters, 1988, **61**(21), pp. 2507–2507, doi: 10.1103/physrevlett.61.2507.

[23] Paulus, G. G., Zacher, F., Walther, H., Lohr, A., Becker, W., and Kleber, M., 'Above-threshold ionization by an elliptically polarized field: Quantum tunneling interferences and classical dodging,' Physical Review Letters, 1998, **80**(3), pp. 484–487, doi:10.1103/physrevlett.80.484.

[24] Paulus, G. G., Grasbon, F., Dreischuh, A., Walther, H., Kopold, R., and Becker, W., 'Above-threshold ionization by an elliptically polarized field: Interplay between electronic quantum trajectories,' Physical Review Letters, 2000, **84**(17), pp. 3791–3794, doi:10.1103/physrevlett.84.3791.

[25] Pfeiffer, A. N., Cirelli, C., Smolarski, M., Dimitrovski, D., Abu-samha, M., Madsen, L. B., and Keller, U., 'Attoclock reveals natural coordinates of the laser-induced tunnelling current flow in atoms,' Nature Physics, 2011, **8**(1), pp. 76–80, doi: 10.1038/nphys2125.

[26] Reiss, H. R., 'Effect of an intense electromagnetic field on a weakly bound system,' Physical Review A, 1980, **22**(5), pp. 1786–1813, doi:10.1103/physreva.22.1786.

[27] Sainadh, U. S., Xu, H., Wang, X., Atia-Tul-Noor, A., Wallace, W. C., Douguet, N., Bray, A., Ivanov, I., Bartschat, K., Kheifets, A., Sang, R. T., and Litvinyuk, I. V., 'Attosecond angular streaking and tunnelling time in atomic hydrogen,' Nature, 2019, **568**(7750), pp. 75–77, doi:10.1038/s41586-019-1028-3.

[28] Sainadh, U. S., Sang, R. T., and Litvinyuk, I. V., 'Attoclock and the quest for tunnelling time in strong-field physics,' Journal of Physics: Photonics, 2020, **2**(4), p. 042002, doi:10.1088/2515-7647/aba009.

[29] Schuricke, M., Zhu, G., Steinmann, J., Simeonidis, K., Ivanov, I., Kheifets, A., Grum-Grzhimailo, A. N., Bartschat, K., Dorn, A., and Ullrich, J., 'Strong-field ionization of lithium,' Physical Review A, 2011, **83**(2), doi:10.1103/physreva.83.023413.

[30] Sharma, S., Acharya, B. P., De Silva, A. H. N. C., Parris, N. W., Ramsey, B. J., Romans, K. L., Dorn, A., de Jesus, V. L. B., and Fischer, D., 'All-optical atom trap as a target for motrims-like collision experiments,' Phys. Rev. A, 2018, **97**, p. 043427, doi:10.1103/PhysRevA.97.043427.

[31] Silva, A. H. N. C. D., Moon, T., Romans, K. L., Acharya, B. P., Dubey, S., Foster, K., Russ, O., Rischbieter, C., Douguet, N., Bartschat, K., and Fischer, D., 'Circular dichroism in atomic resonance-enhanced few-photon ionization,' Physical Review A, 2021, **103**(5), p. 053125, doi:10.1103/physreva.103.053125.

[32] Taïeb, R., Véniard, V., Maquet, A., Manakov, N. L., and Marmo, S. I., 'Circular dichroism from unpolarized atoms in multiphoton multicolor ionization,' Physical Review A, 2000, **62**(1), doi:10.1103/physreva.62.013402.

[33] Thini, F., Romans, K. L., Acharya, B. P., de Silva, A. H. N. C., Compton, K., Foster, K., Rischbieter, C., Russ, O., Sharma, S., Dubey, S., and Fischer, D., 'Photo-ionization of polarized lithium atoms out of an all-optical atom trap: a complete experiment,' Journal of Physics B: Atomic, Molecular and Optical Physics, 2020, **53**(9), p. 095201, doi:10.1088/1361-6455/ab7671.

[34] Wang, Z.-M. and Elliott, D. S., 'Complete measurements of two-photon ionization of atomic rubidium using elliptically polarized light,' Phys. Rev. A, 2000, **62**, p. 053404, doi:10.1103/PhysRevA.62.053404.

[35] Wang, Z.-M. and Elliott, D. S., 'Determination of cross sections and continuum phases of rubidium through complete measurements of atomic multiphoton ionization,' Physical Review Letters, 2000, **84**(17), pp. 3795–3798, doi:10.1103/physrevlett.84.3795.

[36] Zhu, G., Schuricke, M., Steinmann, J., Albrecht, J., Ullrich, J., Ben-Itzhak, I., Zouros, T. J. M., Colgan, J., Pindzola, M. S., and Dorn, A., 'Controlling two-electron threshold dynamics in double photoionization of lithium by initial-state preparation,' Physical Review Letters, 2009, **103**(10), p. 103008, doi:10.1103/physrevlett.103.103008.

II. TWO-PATH INTERFERENCE IN THE RESONANCE-ENHANCED FEW-PHOTON IONIZATION OF ATOMS

B.P.Acharya[1], *S.Dubey*[1], *K.L.Romans*[1], *A.H.N.C.DeSilva*[1], *K.Foster*[1], *O.Russ*[1], *K.Bartschat*[3], *N.Douguet*[2], and *D.Fischer*[1]

[1]Department of Physics Missouri University of Science and Technology
Rolla, Missouri 65409

[2]Department of Physics Kennesaw State University
Kennesaw, Georgia 30144, USA

[3]Department of Physics and Astronomy Drake University
Des Moines, Iowa 50311, USA

ABSTRACT

We investigate the resonance-enhanced few-photon ionization of an atomic Li target at a photon energy near the resonance between the $2s$ ground and $2p$ excited states. For this system, the ground state ionization resembles an atomic "double slit", because it can proceed through the $2p$ resonances with the magnetic quantum number m_ℓ being either -1 or $+1$. In our experiment, the target can be state prepared in one of the polarized excited $2p$ states before subjecting it to the ionizing radiation, thereby effectively closing one of the two slits. This allows to extract the interference term between the two pathways and obtain complex phase information on the final state. The analysis of our experimental results is supported by an *ab initio* model based on the numerical solution of the time-dependent Schrödinger equation.

1. INTRODUCTION

Two-path interference is one of the most intriguing and intensely studied phenomena in physics, which was first discovered in 1801 for optical light by Thomas Young in his double-slit experiment [42]. Its historic importance for the development of quantum theory

cannot be overrated, because it reveals the wave nature of massive particles such as electrons [10, 24], atoms [25], and even large molecules [3] thereby supporting de Broglie's hypothesis of wave-particle duality [11]. Until today, this phenomenon didn't loose its appeal, and it has been observed in numerous systems. On the one hand, it allows to extract phase information, which is commonly not directly observable. On the other hand, it is exploited in many quantum-control schemes, because the manipulation of the relative amplitudes of the two pathways allows to control of the final state with high sensitivity. In atomic and molecular scattering processes, examples include well-known effects like Feshbach, shape, and Fano resonances (e.g. [8, 16, 17, 34]), or atomic-scale double slits formed by diatomic molecules exhibiting interferences in differential ionization cross sections due to ion [14, 30, 38, 43], electron [28, 29], or photon impact [9, 27].

Multiphoton ionization processes of single atoms expose two- and multi-path interferences in a particularly clean way, because of the well-defined energy and limited angular momentum transfer in photon absorption reactions. A prominent example is RABBITT spectroscopy (Reconstruction of Attosecond Beating by Interference of Two-Photon Transitions) [6, 23, 26, 31], which is a common tool to characterize extreme-ultraviolet (XUV) attosecond pulse trains and study attosecond atomic dynamics in the time domain. Two-color ionization schemes using (lower) harmonic radiation [7, 15, 19, 41] enable the coherent control of the reactions' final state via two-path interferences. Recently, other schemes have been considered where double-slit structures in so-called Kramers-Henneberg states emerge by the distortion of bound state in the external field resulting in interference patterns [21]. Two-path interference has not only been observed in laser pulses but also using two mutually incoherent (i.e. without mutual phase lock) continuous-wave (cw) lasers in the two-photon ionization of Rubidium atoms [33], where the photon energies are tuned to two different resonances.

In the present study, two-path interference occurs in the ground state ionization of lithium exposed to single-color femtosecond laser pulses, which are linearly polarized in the y-direction. The laser spectrum has its center wavelength at 665 nm and overlaps with the $2s$–$2p$ resonance at 671 nm. For the quantization axis in the z-direction, the absorption of a single photon results in the excitation to the $2p$ state coherently populating the two magnetic sub-levels with $m_\ell = +1$ and -1. These two eigenstates resemble the two "slits" in analogy to Young's double-slit scheme (see Figure. 1). From these two excited levels, the atom is ionized without further resonance-enhancement by the absorption of two more photons from the same laser pulse resulting in a final superposition of electronic p and f continuum waves.
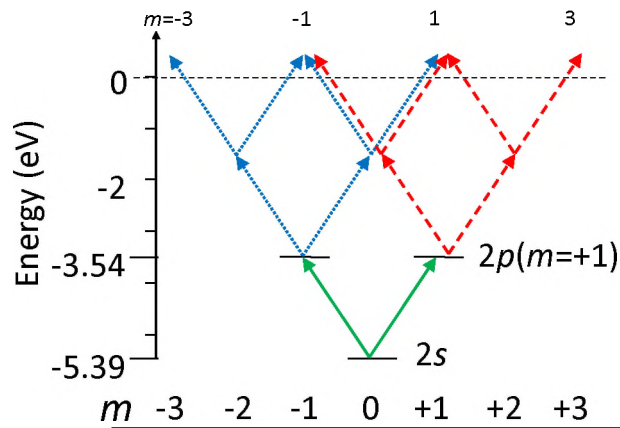
Figure 1. Few-photon ionization scheme in the lowest-order perturbation theory. The ionization pathways from the $2p$ state with $m_\ell = +1$ and -1 are shown as red dashed and blue dotted arrows, respectively. The $2s$ ionization corresponds to the superposition of both.

It is important to note that the distinction of these two pathways relies on the choice of the quantization direction. However, this choice is motivated by the experimental capability of preparing the atoms selectively in one of the two excited and polarized magnetic sub-levels of the $2p$ state before exposing them to the femtosecond laser pulse. This enables us to measure not only the final intensity of the two interfering pathways, which corresponds

to the differential cross sections for the ionization of the $2s$ state, but also the intensity of each pathway individually, which are the cross sections of $2p$ ionization. This can be approximated in the simple equation

$$
\begin{aligned}
|A \cdot \psi_{2s}|^2 &= |\psi_+ + \psi_-|^2 \\
&= |\psi_+|^2 + |\psi_-|^2 + 2\,|\psi_+|\,|\psi_-|\cos\Delta\varphi
\end{aligned}
\tag{1}
$$

where ψ_{2s}, ψ_+, and ψ_- represent the electronic continuum wave functions for the ionization of the initial $2s(m_\ell = 0)$, $2p(m_\ell = +1)$, and $2p(m_\ell = -1)$, respectively. The factor A accounts for the fact that the first excitation step from the initial $2s$ state to the intermediate $2p$ levels modifies the overall ionization probability.

It should be noted that the picture developed here represents an approximation, because the time-dependent population dynamics is not fully accounted for. However, it will be shown below that the experimental observations and model calculations presented here are in very good agreement with the two-path picture outlined above. Eq. 1 provides a direct and intuitive way to extract the phase difference $\Delta\varphi$ between the continuum waves ψ_+ and ψ_- from the measured cross sections, thereby revealing the effect of the orientation of the initial electron orbital angular momentum on the final state's phase.

2. METHODS

The experimental technique and the theoretical methods are identical to those reported in previous studies on very similar systems [1, 12, 37]. Therefore, only some key features are repeated here and parameters specific to the present study are mentioned.

Lithium atoms are cooled and confined in a volume of about 1 mm diameter in a near-resonant all-optical atom trap (AOT) [36] with a fraction of about 25 % being in the polarized excited $2p(m_\ell=+1)$ state and about 75 % in the $2s$ ground state. The atoms are

ionized in the field of a femtosecond laser based on a Ti:Sa oscillator with two non-collinear optical parametric amplifier (NOPA) stages. For the present study, the laser wavelength was chosen to center at 665 nm with pulse durations of about 65 fs and peak intensities up to 10^{12} W/cm^2. The three-dimensional electron momentum vectors are measured with a resolution of about 0.01 a.u. [39] in a reaction microscope (e.g. [18, 22]). It is important to note that this experiment allows to obtain differential cross-normalized data for the ionization of the $2s$ and the $2p$ initial states simultaneously.

In our theoretical model, the lithium atoms are approximated as a single active electron in a $1s^2$ ionic core described by a static Hartree potential [2, 35] supplemented with phenomenological terms [12]. The (complex) final state wave function is obtained by propagating the system numerically solving the time-dependent Schrödinger equation (TDSE).

3. RESULTS AND DISCUSSION

In the present study, lithium atoms in the $2s$ ground state and $2p$ excited state are ionized in a laser field of a wavelength of 665 nm at peak intensities below 10^{12} W/cm^2. This situation corresponds to Keldysh parameters larger than 7 and the system is expected to be well-described in a multi-photon picture. The two initial states are ionized by the absorption of (at least) three or two photons, respectively, resulting in a final electron energy of about 200 meV. The measured electron momentum and energy spectra are shown in Figure. 2 for three different laser intensities. Before proceeding to the analysis of the two-path interference introduced above, three important features of the data should be mentioned that were reported already previously in several recent studies [1, 12]:

First, the final electron energy depends on the laser intensity and even a small second peak can be identified for $2s$ ionization at the highest investigated intensity. Such intensity dependent energy shifts and splittings were reported recently [12] for the same system ionized by circularly polarized femtosecond laser light. They are explained by the coupling
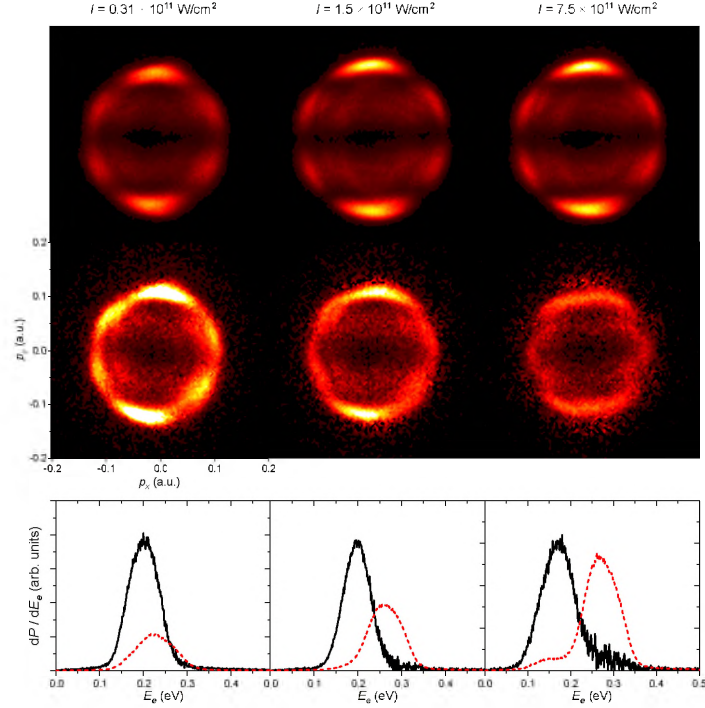
Figure 2. Photoelectron momentum distributions projected to the xy plane for the few-photon ionization of the $2s$ (top row) and $2p(m_\ell{=}{+}1)$ (middle row) initial states by linearly polarized laser pulses of 65 fs duration, at a center wavelength of 665 nm, and with peak intensities of $0.31{\cdot}10^{11}$ W/cm^2 (left), $1.5{\cdot}10^{11}$ W/cm^2 (center), and $7.5{\cdot}10^{11}$ W/cm^2 (right). The laser polarization direction is along the y axis (i.e. vertical), the atomic initial orbital angular momentum is oriented in z direction (perpendicular to the drawing plane). The corresponding photoelectron energy spectra are shown in the bottom row. Here, the cross sections for $2s$ (red dashed line) and $2p$ ionization (solid black line) are cross-normalized in each graph.

of the $2s$ and $2p$ state in the external field resulting in an Autler-Townes splitting [4] of each of these levels. This effect was even considered to be exploited as a femtosecond timescale energy switch of a spin-polarized electron source [12].

Second, while the photoelectron momentum distributions for $2s$ ionization features reflection symmetry with respect to the laser electric field direction (the vertical direction in the momentum spectra shown in Figure. 2), this symmetry is broken for the ionization of the polarized $2p$ state and the main electron emission direction appears to be shifted. This phenomenon is known as magnetic dichroism and its dependence on the laser wavelength and intensity was recently investigated by Acharya *et al.* [1]. In this earlier study, these

asymmetries were explained in a partial wave picture, and two requirements were identified: On the one hand, the final state orbital angular momentum needs to feature a non-vanishing mean orientation $\langle m \rangle \neq 0$, i.e. some information on the initial target polarization needs to be preserved throughout the ionization process. On the other hand, two or more orbital angular momenta ℓ need to interfere in the final state, because they introduce complex phase shifts between the contributing partial waves which give rise to shifts in the photoelectron angular distributions.

And third, the azimuthal photoelectron angular distributions for $2p$ ionization features 6 peaks, which is in direct contradiction to the lowest-order perturbation theory (LOPT). Generally, the dependence of the differential cross sections on the azimuthal angle φ is given by [1]

$$\frac{d\sigma}{d\Omega} = \left| \sum_{m_\ell} c_{m_\ell} e^{im_\ell \varphi} \right|^2 \qquad (2)$$

where the factors c_{m_ℓ} relate to the complex amplitudes of the partial waves. In the LOPT, the absorption of only the minimum number of photons is considered. For the present initial $2p(m_\ell=+1)$ state, this corresponds to the two-photon absorption, which – in the electric dipole approximation – results in partial waves with $m_\ell = -1$, 1, and 3 contributing to the final state (cf. Figure. 1). It is straight-forward to show that for this set of dipole-allowed m_ℓ the above expression results in a photoelectron angular distribution with not more than 4 peaks. This evident violation of LOPT close to the $2s$–$2p$ resonance was reported and discussed in the previous study, too: Again, it is explained by the coupling between the $2s$ and $2p$ states in the external field giving rise to Rabi oscillations between these two states and resulting in a contribution of $m_\ell = -3$ to the final state. Accounting for this additional contribution, the expression in Eq. 2 allows for angular distributions with up to 6 peaks, which is consistent with the experimental observations.

In order to analyze two-path interference, we first study the final state wave functions using our theoretical model for the lowest investigated intensity. Figure. 3 shows photoelectron momentum distributions for $2p$ and $2s$ ionization as well as final state phase information for the former process considering only electron emission in the xy plane (i.e. for a polar angle $\vartheta = 0$). For $2s$ ionization, measured and calculated spectra are consistent featuring a six-peak ring structure, which is symmetric with respect to the laser polarization direction. For $2p$ ionization, there are some discrepancies. Specifically, the angular shift due to magnetic dichroism is larger and the six-peak structure is more pronounced in the measured data. Generally, such differences are not surprising, because of the non-uniform spatial intensity distribution of the laser field around the focal point in the experiment, which results in an averaging over an intensity range in the measured data. This effect was accounted for in previous studies (e.g. [12]) by convoluting calculated spectra over an estimated laser intensity distribution. While this procedure yields excellent agreement between theory and experiment, we opted for not applying this (incoherent) averaging here, because the present interest is focused on the complex phase information, where a rigorous consideration of this averaging effect is not straight-forward.

In Figure. 3 (bottom, left), the complex phase of the final state wave function ψ_+ for $2p(m_\ell=+1)$ ionization is shown. Generally, it varies between $-\pi$ and π and depends on both, the energy and the emission direction of the photoelectron. It is important to note that the plotted phase information is only meaningful, where the intensity of the wave function is significant. This corresponds to the region around a momentum of about 0.1 a.u.. While the phase oscillates very fast at smaller and larger momenta, it changes comparably slow with energy within this range, and it covers three 2π-cycles for the full range of the azimuthal angle φ, which is consistent with Eq. 2.

It is important to note that the two-path interference in Eq. 1 does not directly depend on the phase of ψ_+ plotted in Figure. 3 (bottom, left), but it is rather contingent on the phase difference $\Delta\phi$ between the final states ψ_+ and ψ_- for opposing initial target
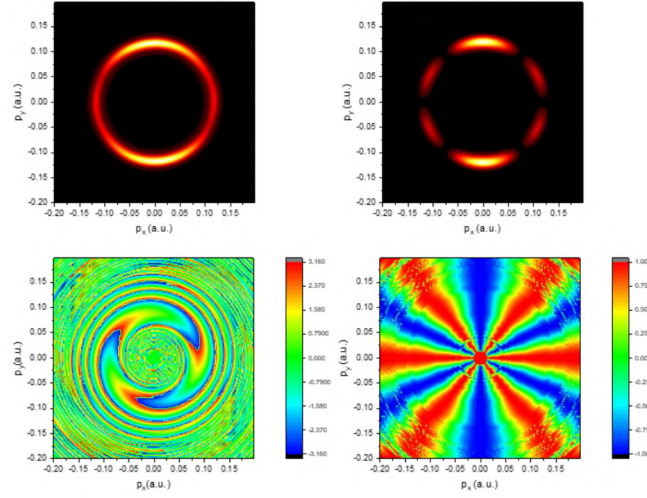
Figure 3. (Top row) Calculated photoelectron momentum distributions in the xy plane for ionization of the $2p(m_\ell=+1)$ (left) and $2s$ (right) initial states. (Bottom row) complex phase of the final state wave function ψ_+ for ionization of the $2p(m_\ell=+1)$ initial state (left), and cosine of the phase difference between ψ_+ and ψ_- (right).

polarizations. This phase difference can be calculated by exploiting the fact that the systems with opposing initial orbital angular momentum $m_\ell = +1$ and -1 are mirror images of one another, and it is $\psi_+(\varphi) = \psi_-(-\varphi)$. The obtained cosine of the phase difference $\cos \Delta\phi$ is plotted in Figure. 3 (bottom, right). Interestingly, it shows only a marginal dependence on the photoelectron energy. In the direction of the azimuthal angle φ in contrast, it undergoes six full oscillations. The validity of the two-path interference picture formulated in Eq. 1 can now be tested by comparing the calculated momentum distribution for $2s$ ionization (corresponding to $|\psi_{2s}|^2$) with the intensity of the superposition of the two wave functions for $2p$ ionization $|\psi_+ + \psi_-|^2$. The momentum distributions obtained by these two different methods are shown in Figure. 4 and are in excellent agreement with each other.

In the discussion above it is shown that the final momentum distribution for $2s$ ionization (which corresponds to $|\psi_{2s}|^2$) can be calculated using the (complex) information of the final state wave function ψ_+ of a different process, namely of the ionization of the polarized $2p(m_\ell=+1)$ initial state. It is important to note that this is not possible with the
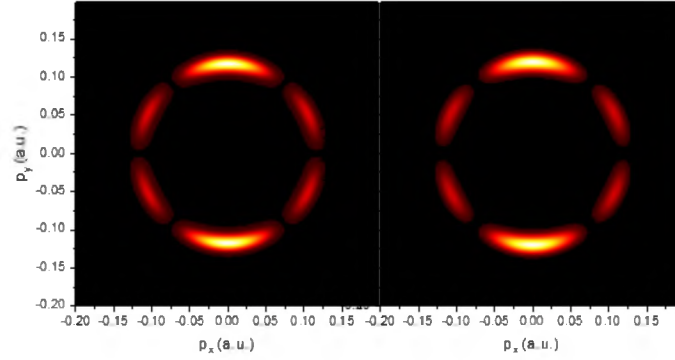
Figure 4. Intensity of the interfering final state wave function for $2p$ ionization with initial magnetic quantum numbers $m_\ell = -1$ and $+1$ (left). Calculated momentum distribution for $2s$ ionization (right) (same as Figure. 3, top right).

experimental data, because only the absolute square of the final state wave function ψ_+ is directly measured, but not its phase. However, the relative phase between ψ_- and ψ_+ can be extracted by reversing the above procedure and solving Eq. 1 for the phase difference, yielding

$$\cos \Delta\phi = \frac{|A \cdot \psi_{2s}|^2 - |\psi_+|^2 - |\psi_-|^2}{2\,|\psi_+|\,|\psi_-|}. \tag{3}$$

Here, the factor A can be determined, because the total flux is conserved, i.e. – in terms of the well-known picture of Young's double slit – the final total intensity has to equal the sum of intensities going through each slit individually. Therefore, the interference term does not change the total intensity and the factor A must fulfill the condition $\int d^3p\,|A\psi_{2s}|^2 = \int d^3p\left(|\psi_-|^2 + |\psi_+|^2\right)$.

Equation 3 can now be employed in order to calculate the phase difference $\Delta\phi$ from the experimental data. However, using fully differential data yields unsatisfactory results, because the photoelectron energy differs slightly for the ionization of the $2s$ and $2p$ states owing to the slight detuning of the femtosecond laser frequency from the $2s$–$2p$ resonance (see Figure. 2). However, the theoretical analysis above showed that the phase difference
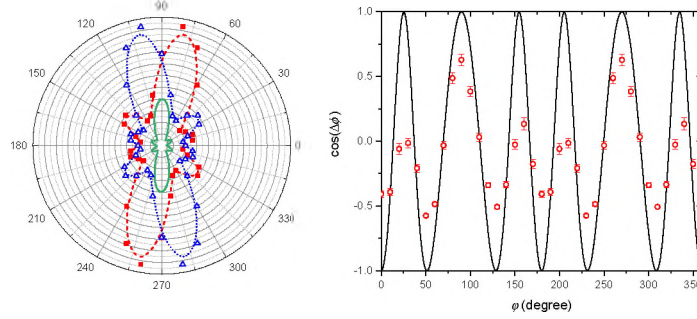
Figure 5. (Left) Experimental photoelectron angular distributions as a function of the azimuthal angle φ for the few-photon ionization of lithium initially in the $2s$ (solid green line) and $2p$ state with $m_\ell = +1$ (red dashed line and solid squares) and -1 (blue dotted line and open triangles). The lines are basis splines to guide the eye. (Right) Experimental and theoretical cosine of the phase difference $\cos \Delta\phi$ as a function of the photoelectron azimuthal angle φ.

does not depend on the photoelectron energy, but only on its azimuthal angle (see Figure. 3, bottom right). Therefore, angular differential data integrated over the photoelectron energy suffices to calculate the phase difference.

The experimental photoelectron angular distributions are shown in Figure. 5 (left). While the distributions for the ionization for the $2s$ and the $2p(m_\ell=+1)$ initial states are measured directly in our experiment, the data for $2p(m_\ell=-1)$ is obtained by reflecting the data for the opposite target polarization on the laser polarization axis. Using these angular distributions, the phase difference is calculated with Eq. 3, plotted in Figure. 5 (right), and compared to the theoretical model. The distribution features six crests and troughs whose positions agree very well for theory and experiment. However, some discrepancies are observed in the magnitude. While the calculated curve reaches the maximum and minimum values of $+1$ and -1, respectively, the oscillation is weaker in the experimental data. Generally, a value of $+1$ for $\cos \Delta\phi$ corresponds to the maximum constructive interference which is expected at angles where the angular distribution for $2s$ ionization has a local maximum. Correspondingly, $\cos \Delta\phi = -1$ means maximum destructive interference, which should occur at local minima in the differential $2s$ ionization data. There are two effects that might blur these interferences in the experimental data: First, a small but non-negligible exper-

imental angular uncertainty contributes. And second, the experimental data represent an average over a laser intensity range, as already discussed above. As the angular distributions are not independent of the laser intensity (see Figure. 2), this will also result in a blurring of the distribution. Overall, the phase differences obtained from the experimental data are consistent with our theoretical model, thereby supporting the validity of the two-path picture developed here.

4. CONCLUSION

In conclusion, we studied the details of electron emission in few-photon ionization of lithium atoms initially either in the $2s$ ground state or in the polarized $2p(m_\ell=+1)$ excited state by radiation close to the 2s–2p resonance. We exploited the fact that the 2s state can be ionized through two possible pathways, specifically through the $2p$ resonance with either $m_\ell = +1$ or -1. These two pathways interfere in the final state and resemble a double-slit. Because our experiment allows to obtain the differential cross sections for the $2s$ and the $2p$ initial states separately, we are able measure the final wave with both "slits" open, or with one "slit" closed. Therefore, the data allow to extract the interference term, thereby providing information on the phase factors of the wave functions. The obtained phases are in good agreement with our theoretical model.

Moreover, several interesting features are observed in the present data, which were reported for similar systems in preceding studies: First, the $2s$ and $2p$ energy levels experience a splitting that depends on the laser intensity due to the Autler-Townes effect. The observed splitting is consistent with previously published data for few-photon ionization of lithium at the same wavelength with circularly polarized light [12]. Second, the photoelectron angular distributions after ionization of the polarized $2p$ state are not symmetric with respect to the laser polarization, but the peaks are shifted. The wavelength and intensity dependence of this effect known as magnetic dichroism was systematically studied in [1]. Moreover, the peak structures in the present angular differential spectra are

in direct contradiction to the lowest-order perturbation theory, which is generally expected to yield reasonable results at the rather moderate intensities used in our experiments. These discrepancies are explained by Rabi oscillations due to the coupling of the 2s and 2p states in the ionizing laser field (see also [1]).

It is worth noting that the present method is not the only way to get access to the final state's phase. The angular distributions can be fitted using model functions described by a superposition of partial waves (cf. Equation. 2), which – under certain conditions – allows to extract the complex amplitudes of the final state. For single-photon ionization, these type of *complete* studies were pioneered in the 1990s using polarized atomic targets [5, 20, 32]. In the multiphoton ionization regime, phase information was obtained by ionizing atoms with elliptically polarized light [13, 40]. However, the present scheme exploiting the resonance enhancement through two magnetic sub-levels provides direct and intuitive access to the interference term and the final phase information.

Two- are multi-path interferences in few-photon ionization are well suited for quantum control schemes, if the relative phases and intensities of the different paths can be regulated (e.g. [19]). It is interesting to conceive such a scheme for the present system. In fact, controlling the relative (complex) amplitudes of the transient $2p(m_\ell=-1)$ and $2p(m_\ell=+1)$ populations is experimentally straight-forward. The transitions from the $2s$ ground state to the two polarized excited $2p$ levels are driven by left- and right-handed circularly polarized laser radiation, respectively, propagating in the z-direction. The superposition of these two fields with equal intensity corresponds to linearly polarized light like it is used in the present experiment. The change of their relative phase corresponds to a rotation of the polarization direction in the xy plane. The change of the relative intensities is achieved by introducing an ellipticity to the radiation. In the present scheme, quasi-monochromatic light is used and changes of the laser polarization would also affect the ionization steps after populating the resonant $2p$ levels. However, the effect on the excitation process and the ultimate ionization could be de-coupled by using bichromatic laser fields with a weak contribution close to

the $2s$–$2p$ resonance and a stronger contribution off resonance. Such an experiment would allow to prepare an atomic target in a coherent superposition of excited magnetic sub-states before ionizing it, thereby providing numerous possibilities to analyze and control the final state.

ACKNOWLEDGEMENTS

REFERENCES

[1] Acharya, B. P., Dobson, M., Dubey, S., Romans, K. L., Silva, A. H. N. C. D., Foster, K., Russ, O., Bartschat, K., Douguet, N., and Fischer, D., 'Magnetic dichroism in the few-photon ionization of polarized atoms,' Physical Review A, to be submitted.

[2] Albright, B. J., Bartschat, K., and Flicek, P. R., 'Core potentials for quasi-one-electron systems,' Journal of Physics B: Atomic, Molecular and Optical Physics, 1993, **26**(3), pp. 337–344, doi:10.1088/0953-4075/26/3/008.

[3] Arndt, M., Nairz, O., Vos-Andreae, J., Keller, C., van der Zouw, G., and Zeilinger, A., 'Wave–particle duality of c60 molecules,' Nature, 1999, **401**(6754), pp. 680–682, doi:10.1038/44348.

[4] Autler, S. H. and Townes, C. H., 'Stark effect in rapidly varying fields,' Physical Review, 1955, **100**(2), pp. 703–722, doi:10.1103/physrev.100.703.

[5] Becker, U., 'Complete photoionisation experiments1dedicated to professor h. kleinpoppen, stirling, for his 70th birthday.1,' Journal of Electron Spectroscopy and Related Phenomena, 1998, **96**(1), pp. 105 – 115, ISSN 0368-2048, doi: https://doi.org/10.1016/S0368-2048(98)00226-6.

[6] Bharti, D., Atri-Schuller, D., Menning, G., Hamilton, K. R., Moshammer, R., Pfeifer, T., Douguet, N., Bartschat, K., and Harth, A., 'Decomposition of the transition phase in multi-sideband schemes for reconstruction of attosecond beating by interference of two-photon transitions,' Physical Review A, 2021, **103**(2), p. 022834, doi:10.1103/physreva.103.022834.

[7] Brif, C., Chakrabarti, R., and Rabitz, H., 'Control of quantum phenomena: past, present and future,' New Journal of Physics, 2010, **12**(7), p. 075008, doi:10.1088/1367-2630/12/7/075008.

[8] Chin, C., Grimm, R., Julienne, P., and Tiesinga, E., 'Feshbach resonances in ultracold gases,' Reviews of Modern Physics, 2010, **82**(2), pp. 1225–1286, doi: 10.1103/revmodphys.82.1225.

[9] Cohen, H. D. and Fano, U., 'Interference in the photo-ionization of molecules,' Physical Review, 1966, **150**(1), pp. 30–33, doi:10.1103/physrev.150.30.

[10] Davisson, C. J. and Germer, L. H., 'Reflection of electrons by a crystal of nickel,' Proceedings of the National Academy of Sciences, 1928, **14**(4), pp. 317–322, doi: 10.1073/pnas.14.4.317.

[11] de Broglie, L., 'Thèse de doctorat (masson, paris, 1924),' J. Physique (serie 6), 1927, **VIII**, p. 225.

[12] De Silva, A. H. N. C., Moon, T., Romans, K. L., Acharya, B. P., Dubey, S., Foster, K., Russ, O., Rischbieter, C., Douguet, N., Bartschat, K., and Fischer, D., 'Circular dichroism in atomic resonance-enhanced few-photon ionization,' Phys. Rev. A, 2021, **103**, p. 053125, doi:10.1103/PhysRevA.103.053125.

[13] Dulieu, F., Blondel, C., and Delsart, C., 'Multiphoton angular distributions with elliptically polarized light. i. analytic ellipticity dependence of photoelectron distributions in the polarization plane,' Journal of Physics B: Atomic, Molecular and Optical Physics, 1995, **28**(17), pp. 3845–3859, doi:10.1088/0953-4075/28/17/021.

[14] Egodapitiya, K. N., Sharma, S., Hasan, A., Laforge, A. C., Madison, D. H., Moshammer, R., and Schulz, M., 'Manipulating atomic fragmentation processes by controlling the projectile coherence,' Physical Review Letters, 2011, **106**(15), p. 153202, doi:10.1103/physrevlett.106.153202.

[15] Ehlotzky, F., 'Atomic phenomena in bichromatic laser fields,' Physics Reports, 2001, **345**(4), pp. 175–264, doi:10.1016/s0370-1573(00)00100-9.

[16] Fano, U., 'Effects of configuration interaction on intensities and phase shifts,' Physical Review, 1961, **124**(6), pp. 1866–1878, doi:10.1103/physrev.124.1866.

[17] Feshbach, H., 'Unified theory of nuclear reactions,' Annals of Physics, 1958, **5**(4), pp. 357–390, doi:10.1016/0003-4916(58)90007-1.

[18] Fischer, D., 'Recoil ion momentum spectroscopy with laser-cooled targets,' 2019, pp. 103–156, doi:10.1515/9783110580297-006.

[19] Giannessi, L., Allaria, E., Prince, K. C., Callegari, C., Sansone, G., Ueda, K., Morishita, T., Liu, C. N., Grum-Grzhimailo, A. N., Gryzlova, E. V., Douguet, N., and Bartschat, K., 'Coherent control schemes for the photoionization of neon and helium in the extreme ultraviolet spectral region,' Scientific Reports, 2018, **8**(1), doi: 10.1038/s41598-018-25833-7.

[20] Godehusen, K., Zimmermann, P., Verweyen, A., von dem Borne, A., Wernet, P., and Sonntag, B., 'A complete photoionization experiment with polarized atoms using magnetic dichroism and phase tilt measurements,' Phys. Rev. A, 1998, **58**, pp. R3371–R3374, doi:10.1103/PhysRevA.58.R3371.

[21] He, P.-L., Zhang, Z.-H., and He, F., 'Young's double-slit interference in a hydrogen atom,' Physical Review Letters, 2020, **124**(16), p. 163201, doi: 10.1103/physrevlett.124.163201.

[22] Hubele, R., Schuricke, M., Goullon, J., Lindenblatt, H., Ferreira, N., Laforge, A., Brühl, E., de Jesus, V. L. B., Globig, D., Kelkar, A., Misra, D., Schneider, K., Schulz, M., Sell, M., Song, Z., Wang, X., Zhang, S., and Fischer, D., 'Electron and recoil ion momentum imaging with a magneto-optically trapped target,' Review of Scientific Instruments, 2015, **86**(3), p. 033105, doi:10.1063/1.4914040.

[23] Isinger, M., Squibb, R. J., Busto, D., Zhong, S., Harth, A., Kroon, D., Nandi, S., Arnold, C. L., Miranda, M., Dahlström, J. M., Lindroth, E., Feifel, R., Gisselbrecht, M., and L'Huillier, A., 'Photoionization in the time and frequency domain,' Science, 2017, **358**(6365), pp. 893–896, doi:10.1126/science.aao7043.

[24] Jönsson, C., 'Elektroneninterferenzen an mehreren künstlich hergestellten feinspalten,' Zeitschrift für Physik, 1961, **161**(4), pp. 454–474, doi:10.1007/bf01342460.

[25] Keith, D. W., Ekstrom, C. R., Turchette, Q. A., and Pritchard, D. E., 'An interferometer for atoms,' Physical Review Letters, 1991, **66**(21), pp. 2693–2696, doi: 10.1103/physrevlett.66.2693.

[26] Klünder, K., Dahlström, J. M., Gisselbrecht, M., Fordell, T., Swoboda, M., Guénot, D., Johnsson, P., Caillat, J., Mauritsson, J., Maquet, A., Taïeb, R., and L'Huillier, A., 'Probing single-photon ionization on the attosecond time scale,' Physical Review Letters, 2011, **106**(14), p. 143002, doi:10.1103/physrevlett.106.143002.

[27] Kunitski, M., Eicke, N., Huber, P., Köhler, J., Zeller, S., Voigtsberger, J., Schlott, N., Henrichs, K., Sann, H., Trinter, F., Schmidt, L. P. H., Kalinin, A., Schöffler, M. S., Jahnke, T., Lein, M., and Dörner, R., 'Double-slit photoelectron interference in strong-field ionization of the neon dimer,' Nature Communications, 2019, **10**(1), doi:10.1038/s41467-018-07882-8.

[28] Li, X., Ren, X., Hossen, K., Wang, E., Chen, X., and Dorn, A., 'Two-center interference in electron-impact ionization of molecular hydrogen,' Physical Review A, 2018, **97**(2), p. 022706, doi:10.1103/physreva.97.022706.

[29] Milne-Brownlie, D. S., Foster, M., Gao, J., Lohmann, B., and Madison, D. H., 'Young-type interference in(e,2e)ionization ofH2,' Physical Review Letters, 2006, **96**(23), p. 233201, doi:10.1103/physrevlett.96.233201.

[30] Misra, D., Kadhane, U., Singh, Y. P., Tribedi, L. C., Fainstein, P. D., and Richard, P., 'Interference effect in electron emission in heavy ion collisions withH2detected by comparison with the measured electron spectrum from atomic hydrogen,' Physical Review Letters, 2004, **92**(15), p. 153201, doi:10.1103/physrevlett.92.153201.

[31] Muller, H., 'Reconstruction of attosecond harmonic beating by interference of two-photon transitions,' Applied Physics B, 2002, **74**(S1), pp. s17–s21, doi: 10.1007/s00340-002-0894-8.

[32] Pahler, M., Lorenz, C., Raven, E. v., Rüder, J., Sonntag, B., Baier, S., Müller, B. R., Schulze, M., Staiger, H., Zimmermann, P., and Kabachnik, N. M., 'Angle-dependent photoelectron spectroscopy of laser-aligned atoms: Li,' Phys. Rev. Lett., 1992, **68**, pp. 2285–2288, doi:10.1103/PhysRevLett.68.2285.

[33] Pursehouse, J., Murray, A. J., Wätzel, J., and Berakdar, J., 'Dynamic double-slit experiment in a single atom,' Physical Review Letters, 2019, **122**(5), p. 053204, doi:10.1103/physrevlett.122.053204.

[34] Schulz, G. J., 'Resonances in electron impact on atoms,' Reviews of Modern Physics, 1973, **45**(3), pp. 378–422, doi:10.1103/revmodphys.45.378.

[35] Schuricke, M., Zhu, G., Steinmann, J., Simeonidis, K., Ivanov, I., Kheifets, A., Grum-Grzhimailo, A. N., Bartschat, K., Dorn, A., and Ullrich, J., 'Strong-field ionization of lithium,' Physical Review A, 2011, **83**(2), doi:10.1103/physreva.83.023413.

[36] Sharma, S., Acharya, B. P., De Silva, A. H. N. C., Parris, N. W., Ramsey, B. J., Romans, K. L., Dorn, A., de Jesus, V. L. B., and Fischer, D., 'All-optical atom trap as a target for motrims-like collision experiments,' Phys. Rev. A, 2018, **97**, p. 043427, doi:10.1103/PhysRevA.97.043427.

[37] Silva, A. H. N. C. D., Moon, T., Romans, K. L., Acharya, B. P., Dubey, S., Foster, K., Russ, O., Rischbieter, C., Douguet, N., Bartschat, K., and Fischer, D., 'Circular dichroism in atomic resonance-enhanced few-photon ionization,' Physical Review A, 2021, **103**(5), p. 053125, doi:10.1103/physreva.103.053125.

[38] Stolterfoht, N., Sulik, B., Hoffmann, V., Skogvall, B., Chesnel, J. Y., Rangama, J., Frémont, F., Hennecart, D., Cassimi, A., Husson, X., Landers, A. L., Tanis, J. A., Galassi, M. E., and Rivarola, R. D., 'Evidence for interference effects in electron emission fromH2colliding with60mev/uKr34 ions,' Physical Review Letters, 2001, **87**(2), p. 023201, doi:10.1103/physrevlett.87.023201.

[39] Thini, F., Romans, K. L., Acharya, B. P., de Silva, A. H. N. C., Compton, K., Foster, K., Rischbieter, C., Russ, O., Sharma, S., Dubey, S., and Fischer, D., 'Photo-ionization of polarized lithium atoms out of an all-optical atom trap: a complete experiment,' Journal of Physics B: Atomic, Molecular and Optical Physics, 2020, **53**(9), p. 095201, doi:10.1088/1361-6455/ab7671.

[40] Wang, Z.-M. and Elliott, D. S., 'Determination of cross sections and continuum phases of rubidium through complete measurements of atomic multiphoton ionization,' Physical Review Letters, 2000, **84**(17), pp. 3795–3798, doi:10.1103/physrevlett.84.3795.

[41] Yin, Y.-Y., Chen, C., Elliott, D. S., and Smith, A. V., 'Asymmetric photoelectron angular distributions from interfering photoionization processes,' Physical Review Letters, 1992, **69**(16), pp. 2353–2356, doi:10.1103/physrevlett.69.2353.

[42] Young, T., 'On the theory of light and colours,' Philosophical Transactions of the Royal Society of London, 1802, **92**, p. 12.

[43] Zhang, S., Fischer, D., Schulz, M., Voitkiv, A., Senftleben, A., Dorn, A., Ullrich, J., Ma, X., and Moshammer, R., 'Two-center interferences in dielectronic transitions inH2HeCollisions,' Physical Review Letters, 2014, **112**(2), p. 023201, doi:10.1103/physrevlett.112.023201.

SECTION

3. SUMMARY AND CONCLUSIONS

This dissertation contains the description of newly developed experimental tools using the most advanced methods available in atomic, molecular, and optical physics to achieve the control as well as analysis of the systems under investigation. First, we developed an all-optical atom trap (AOT) to confine a gaseous lithium atom sample in a small volume in an ultra-high vacuum chamber and cool it down to temperatures in the millikelvin range. The AOT operates with lasers near the 2s-2p resonance of lithium and leaves about 25 % of the atoms in the excited and polarized $2p(m_\ell=+1)$ state. Second, these atoms are subjected to intense laser radiation. To this end, we implemented a femtosecond laser source providing pulses at tunable optical frequencies with pulse durations between 65 and 8 fs and intensities of typically about 10^{11}-10^{12} W/cm^2. And third, in order to characterize the fragmentation of the atoms in the intense laser field we employed an electron and ion momentum spectrometer measuring the three-dimensional momentum vectors of the lithium fragments after ionization processes.

These experimental tools were used in several measurements studying two-, three, and four-photon ionization of lithium by linearly polarized light. The target initial state was prepared either in the unpolarized (spherically symmetric) 2s state or in the polarized $2p(m_\ell = +1)$. The data obtained in this experiments revealed several interesting features which are subsumed in two manuscripts:

The first paper deals with symmetry breakings in photo-electron angular distribution (PAD) for the ionization of polarized atoms is observed. For spherically symmetric or randomly oriented targets, the laser polarization direction represents generally a symmetry axis (in the electric dipole approximation). This symmetry is clearly broken for the ionization of

Li(2p, m_ℓ = +1). Similar phenomena occur for the absorption by ferromagnetic materials and are referred to as Magnetic Dichroism (MD). Our experiment represents a particularly clean and fundamental realization of this effect, and we were able to pin the requirements down under whihc such asymmetries occur. Our result expected to impact also so-called "attoclock" experiments, which aim to extract time-delays of the uantum-mechanical tunneling process in the strong-field ionization of atoms.

For the second manuscript, we studied the details of electron emission if the lithium atoms are subjected to radiation close to the 2s–2p resonance (at 670 nm). We observed significant impacts of this resonance on the ionization dynamics: First, the energy levels experience a splitting that depends on the laser intensity due to the Autler-Townes effect. Second, the electron angular distributions after ionization of the excited 2p state feature structures that are in direct contradiction to the lowest-order perturbation theory, which is generally expected to yield reasonable results at the rather moderate intensities used in our experiments. We were able to explain these discrepancies by Rabi oscillations due to the coupling of the 2s and 2p states in the ionizing laser field. And Third, we exploited the fact that the 2s state can be ionized throught two possible pathways, specifically through the 2p resonance with either m_ℓ = +1 or −1. These two pathways interfere in the final state and resemble a double-slit like in the historical optical experiment performed by Thomas Young in 1801. Because our experiment allows to obtain the differential cross sections for the 2s and the 2p initial states separately, we are able measure the final wave with both "slits" open, or with one "slit" closed. These data allow to extract the interference term and, therefore, it provides information on the phase factors of the wave functions. The extracted phases are in good agreement with our theoretical model.

Overall, the new observations deepen our understanding of light matter interaction, they provide insights into fundamental symmetries, and they help to develope and refine tools for the quantum-control of atomic and subatomic particles.

REFERENCES

[1] P. Weinberger, 'Revisiting louis de broglie's famous 1924 paper in the philosophical magazine,' Philosophical Magazine Letters, 2006, **86**(7), pp. 405–410, doi: 10.1080/09500830600876565.

[2] U. Fano, 'Description of states in quantum mechanics by density matrix and operator techniques,' Rev. Mod. Phys., 1957, **29**, pp. 74–93, doi:10.1103/RevModPhys.29.74.

[3] M. C. Standage and H. Kleinpoppen, 'Photon vector polarization and coherence parameters in an electron-photon coincidence experiment on helium,' Phys. Rev. Lett., 1976, **36**, pp. 577–580, doi:10.1103/PhysRevLett.36.577.

[4] O. Plotzke, G. Prümper, B. Zimmermann, U. Becker, and H. Kleinpoppen, 'Magnetic dichroism in the angular distribution of atomic oxygen2pphotoelectrons,' Physical Review Letters, 1996, **77**(13), pp. 2642–2645, doi:10.1103/physrevlett.77.2642.

[5] M. Eminyan, K. B. MacAdam, J. Slevin, and H. Kleinpoppen, 'Measurements of complex excitation amplitudes in electron-helium collisions by angular correlations using a coincidence method,' Phys. Rev. Lett., 1973, **31**, pp. 576–579, doi: 10.1103/PhysRevLett.31.576.

[6] K. L. Reid, 'Photoelectron angular distributions,' Annual Review of Physical Chemistry, 2003, **54**(1), pp. 397–424, doi:10.1146/annurev.physchem.54.011002.103814, pMID: 12574491.

[7] P. Hockett, M. Wollenhaupt, C. Lux, and T. Baumert, 'Complete photoionization experiments via ultrafast coherent control with polarization multiplexing,' Phys. Rev. Lett., 2014, **112**, p. 223001, doi:10.1103/PhysRevLett.112.223001.

[8] N. Cherepkov, 'Complete experiments in photoionization of atoms and molecules,' Journal of Electron Spectroscopy and Related Phenomena, 2005, **144-147**, pp. 1197–1201, ISSN 0368-2048, doi:https://doi.org/10.1016/j.elspec.2005.01.257, proceeding of the Fourteenth International Conference on Vacuum Ultraviolet Radiation Physics.

[9] H. Klar and H. Kleinpoppen, 'Angular distribution of photoelectrons from polarised atoms exposed to polarised radiation,' Journal of Physics B: Atomic and Molecular Physics, 1982, **15**(6), pp. 933–950, doi:10.1088/0022-3700/15/6/019.

[10] H. U, *Angle- and Spin-Resolved Photoelectron Spectroscopy*, Plenum, New York, 1985.

[11] C. Heckenkamp, F. Schäfers, G. Schönhense, and U. Heinzmann, 'Angular dependence of the spin-polarization transfer from circularly polarized synchrotron radiation onto photoelectrons from atomic xe $5p^6$,' Phys. Rev. Lett., 1984, **52**, pp. 421–424, doi:10.1103/PhysRevLett.52.421.

[12] M. Pahler, C. Lorenz, E. v. Raven, J. Rüder, B. Sonntag, S. Baier, B. R. Müller, M. Schulze, H. Staiger, P. Zimmermann, and N. M. Kabachnik, 'Angle-dependent photoelectron spectroscopy of laser-aligned atoms: Li,' Phys. Rev. Lett., 1992, **68**, pp. 2285–2288, doi:10.1103/PhysRevLett.68.2285.

[13] U. Becker, 'Complete photoionisation experiments1dedicated to professor h. klein-poppen, stirling, for his 70th birthday.1,' Journal of Electron Spectroscopy and Related Phenomena, 1998, **96**(1), pp. 105 – 115, ISSN 0368-2048, doi: https://doi.org/10.1016/S0368-2048(98)00226-6.

[14] K. Godehusen, P. Zimmermann, A. Verweyen, A. von demBorne, P. Wernet, and B. Sonntag, 'A complete photoionization experiment with polarized atoms using magnetic dichroism and phase tilt measurements,' Phys. Rev. A, 1998, **58**, pp. R3371–R3374, doi:10.1103/PhysRevA.58.R3371.

[15] G. Zhu, M. Schuricke, J. Steinmann, J. Albrecht, J. Ullrich, I. Ben-Itzhak, T. J. M. Zouros, J. Colgan, M. S. Pindzola, and A. Dorn, 'Controlling two-electron threshold dynamics in double photoionization of lithium by initial-state preparation,' Physical Review Letters, 2009, **103**(10), p. 103008, doi:10.1103/physrevlett.103.103008.

[16] P. O'Keeffe, P. Bolognesi, A. Mihelič, A. Moise, R. Richter, G. Cautero, L. Stebel, R. Sergo, L. Pravica, E. Ovcharenko, P. Decleva, and L. Avaldi, 'Photoelectron angular distributions from polarized ne* atoms near threshold,' Phys. Rev. A, 2010, **82**, p. 052522, doi:10.1103/PhysRevA.82.052522.

[17] T. Mazza, M. Ilchen, A. Rafipoor, C. Callegari, P. Finetti, O. Plekan, K. Prince, R. Richter, A. Demidovich, C. Grazioli, L. Avaldi, P. Bolognesi, M. Coreno, P. O'Keeffe, M. D. Fraia, M. Devetta, Y. Ovcharenko, V. Lyamayev, S. Düsterer, K. Ueda, J. Costello, E. Gryzlova, S. Strakhova, A. Grum-Grzhimailo, A. Bozhevol-nov, A. Kazansky, N. Kabachnik, and M. Meyer, 'Angular distribution and circular dichroism in the two-colour xuv+nir above-threshold ionization of helium,' Journal of Modern Optics, 2016, **63**(4), pp. 367–382, doi:10.1080/09500340.2015.1119897.

[18] M. Ilchen, N. Douguet, T. Mazza, A. J. Rafipoor, C. Callegari, P. Finetti, O. Plekan, K. C. Prince, A. Demidovich, C. Grazioli, L. Avaldi, P. Bolognesi, M. Coreno, M. Di Fraia, M. Devetta, Y. Ovcharenko, S. Düsterer, K. Ueda, K. Bartschat, A. N. Grum-Grzhimailo, A. V. Bozhevolnov, A. K. Kazansky, N. M. Kabachnik, and M. Meyer, 'Circular dichroism in multiphoton ionization of resonantly excited he$^+$ ions,' Phys. Rev. Lett., 2017, **118**, p. 013002, doi:10.1103/PhysRevLett.118.013002.

[19] A. H. N. C. De Silva, T. Moon, K. L. Romans, B. P. Acharya, S. Dubey, K. Foster, O. Russ, C. Rischbieter, N. Douguet, K. Bartschat, and D. Fischer, 'Circular dichroism in atomic resonance-enhanced few-photon ionization,' Phys. Rev. A, 2021, **103**, p. 053125, doi:10.1103/PhysRevA.103.053125.

[20] P. Lambropoulos, 'Topics on multiphoton processes in atoms,' Adv. At. Mol. Phys., 1976, **12**, pp. 87–164, doi:10.1016/s0065-2199(08)60043-3.

[21] M. Meyer, A. N. Grum-Grzhimailo, D. Cubaynes, Z. Felfli, E. Heinecke, S. T. Manson, and P. Zimmermann, 'Magnetic dichroism in k-shell photoemission from laser excited li atoms,' Phys. Rev. Lett., 2011, **107**, p. 213001, doi: 10.1103/PhysRevLett.107.213001.

[22] S. Sharma, B. P. Acharya, A. H. N. C. De Silva, N. W. Parris, B. J. Ramsey, K. L. Romans, A. Dorn, V. L. B. deJesus, and D. Fischer, 'All-optical atom trap as a target for motrims-like collision experiments,' Phys. Rev. A, 2018, **97**, p. 043427, doi:10.1103/PhysRevA.97.043427.

[23] R. Dörner, V. Mergel, O. Jagutzki, L. Spielberger, J. Ullrich, R. Moshammer, and H. Schmidt-Böcking, 'Cold target recoil ion momentum spectroscopy: a 'momentum microscope' to view atomic collision dynamics,' Physics Reports, 2000, **330**(2), pp. 95–192, ISSN 0370-1573, doi:https://doi.org/10.1016/S0370-1573(99)00109-X.

[24] K. H. Moshammer R., Fischer D., *Recoil-Ion Momentum Spectroscopy and "Reaction Microscopes"*, Springer-Verlag Berlin Heidelberg, 2003.

[25] F. Thini, K. L. Romans, B. P. Acharya, A. H. N. C. deSilva, K. Compton, K. Foster, C. Rischbieter, O. Russ, S. Sharma, S. Dubey, and D. Fischer, 'Photo-ionization of polarized lithium atoms out of an all-optical atom trap: a complete experiment,' Journal of Physics B: Atomic, Molecular and Optical Physics, 2020, **53**(9), p. 095201, doi:10.1088/1361-6455/ab7671.

[26] A. H. N. C. D. Silva, T. Moon, K. L. Romans, B. P. Acharya, S. Dubey, K. Foster, O. Russ, C. Rischbieter, N. Douguet, K. Bartschat, and D. Fischer, 'Circular dichroism in atomic resonance-enhanced few-photon ionization,' Physical Review A, 2021, **103**(5), p. 053125, doi:10.1103/physreva.103.053125.

[27] M. Getzlaff, C. Ostertag, G. H. Fecher, N. A. Cherepkov, and G. Schönhense, 'Magnetic dichroism in photoemission with unpolarized light,' Phys. Rev. Lett., 1994, **73**, pp. 3030–3033, doi:10.1103/PhysRevLett.73.3030.

[28] A. Dorn, A. Elliott, J. Lower, E. Weigold, J. Berakdar, A. Engelns, and H. Klar, 'Orientational dichroism in the electron-impact ionization of laser-oriented atomic sodium,' Phys. Rev. Lett., 1998, **80**, pp. 257–260, doi:10.1103/PhysRevLett.80.257.

[29] R. Hubele, M. Schuricke, J. Goullon, H. Lindenblatt, N. Ferreira, A. Laforge, E. Brühl, V. L. B. deJesus, D. Globig, A. Kelkar, D. Misra, K. Schneider, M. Schulz, M. Sell, Z. Song, X. Wang, S. Zhang, and D. Fischer, 'Electron and recoil ion momentum imaging with a magneto-optically trapped target,' Review of Scientific Instruments, 2015, **86**(3), p. 033105, doi:10.1063/1.4914040.

[30] A. Einstein, 'On a heuristic viewpoint concerning the production and transformation of light.' Annalen der Physik, 1905, **17**, pp. 132–148.

[31] H. B. Bebb and A. Gold, 'Multiphoton ionization of hydrogen and rare-gas atoms,' Phys. Rev., 1966, **143**, pp. 1–24, doi:10.1103/PhysRev.143.1.

[32] T. Brabec and F. Krausz, 'Intense few-cycle laser fields: Frontiers of nonlinear optics,' Rev. Mod. Phys., 2000, **72**, pp. 545–591, doi:10.1103/RevModPhys.72.545.

[33] G. vonHelden, I. Holleman, G. M. H. Knippels, A. F. G. van derMeer, and G. Meijer, 'Infrared resonance enhanced multiphoton ionization of fullerenes,' Phys. Rev. Lett., 1997, **79**, pp. 5234–5237, doi:10.1103/PhysRevLett.79.5234.

[34] J. Steinmann, *Multiphoton Ionization of Laser Cooled Lithium*, Ph.D. thesis, University of Heidelberg, Germany, 2007.

[35] G. Mainfray and G. Manus, 'Multiphoton ionization of atoms,' Reports on Progress in Physics, 1991, **54**(10), pp. 1333–1372, doi:10.1088/0034-4885/54/10/002.

[36] G. Drake, *Handbook of Atomic, Molecular, and Optical Physics*, Springer, 2006.

[37] K. J. Schafer, B. Yang, L. F. DiMauro, and K. C. Kulander, 'Above threshold ionization beyond the high harmonic cutoff,' Phys. Rev. Lett., 1993, **70**, pp. 1599–1602, doi:10.1103/PhysRevLett.70.1599.

[38] P. B. Corkum, N. H. Burnett, and F. Brunel, 'Above-threshold ionization in the long-wavelength limit,' Phys. Rev. Lett., 1989, **62**, pp. 1259–1262, doi:10.1103/PhysRevLett.62.1259.

[39] Z. Zhang, M. N. Shneider, and R. B. Miles, 'Coherent microwave rayleigh scattering from resonance-enhanced multiphoton ionization in argon,' Phys. Rev. Lett., 2007, **98**, p. 265005, doi:10.1103/PhysRevLett.98.265005.

[40] L. Zandee and R. B. Bernstein, 'Resonance-enhanced multiphoton ionization and fragmentation of molecular beams: No, i2, benzene, and butadiene,' The Journal of Chemical Physics, 1979, **71**(3), pp. 1359–1371, doi:10.1063/1.438436.

[41] M. Fu, H. Ma, J. Cao, and W. Bian, 'Laser cooling of cabr molecules and production of ultracold br atoms: A theoretical study including spin–orbit coupling,' The Journal of Chemical Physics, 2017, **146**(13), p. 134309, doi:10.1063/1.4979566.

[42] D. J. Jackson, J. J. Wynne, and P. H. Kes, 'Resonance-enhanced multiphoton ionization: Interference effects due to harmonic generation,' Phys. Rev. A, 1983, **28**, pp. 781–794, doi:10.1103/PhysRevA.28.781.

[43] A. D. Silva, D. Atri-Schuller, S. Dubey, B. Acharya, K. Romans, K. Foster, O. Russ, K. Compton, C. Rischbieter, N. Douguet, K. Bartschat, and D. Fischer, 'Using circular dichroism to control energy transfer in multiphoton ionization,' Physical Review Letters, 2021, **126**(2), doi:10.1103/physrevlett.126.023201.

[44] T. Hänsch and A. Schawlow, 'Cooling of gases by laser radiation,' Optics Communications, 1975, **13**(1), pp. 68–69, ISSN 0030-4018, doi:https://doi.org/10.1016/0030-4018(75)90159-5.

[45] H. D. D. J. Wineland, 'Laser cooling,' Bull. Am. Phys. Soc., 1975, **20**, p. 637.

[46] H. J. Metcalf and P. van derStraten, *Laser Cooling and Trapping*, Springer, New York, NY, Springer-Verlag New York, Inc. 1999, 1999.

[47] W. D. Phillips, 'Nobel lecture: Laser cooling and trapping of neutral atoms,' Rev. Mod. Phys., 1998, **70**, pp. 721–741, doi:10.1103/RevModPhys.70.721.

[48] M. H. Anderson, J. R. Ensher, M. R. Matthews, C. E. Wieman, and E. A. Cornell, 'Observation of bose-einstein condensation in a dilute atomic vapor,' Science, 1995, **269**(5221), pp. 198–201, ISSN 0036-8075, doi:10.1126/science.269.5221.198.

[49] K. B. Davis, M. O. Mewes, M. R. Andrews, N. J. vanDruten, D. S. Durfee, D. M. Kurn, and W. Ketterle, 'Bose-einstein condensation in a gas of sodium atoms,' Phys. Rev. Lett., 1995, **75**, pp. 3969–3973, doi:10.1103/PhysRevLett.75.3969.

[50] B. DeMarco and D. S. Jin, 'Onset of fermi degeneracy in a trapped atomic gas,' Science, 1999, **285**(5434), pp. 1703–1706, ISSN 0036-8075, doi: 10.1126/science.285.5434.1703.

[51] D. Fischer, *Recoil ion momentum spectroscopy with laser-cooled targets(Chapter 6)*, Walter de Gruyter GmbH&CoKG, 2006.

[52] A. P. Kazantsev and I. V. Krasnov, 'Rectification effect of a radiation force,' J. Opt. Soc. Am. B, 1989, **6**(11), pp. 2140–2148, doi:10.1364/JOSAB.6.002140.

[53] R. Grimm, Y. B. Ovchinnikov, A. I. Sidorov, and V. S. Letokhov, 'Observation of a strong rectified dipole force in a bichromatic standing light wave,' Phys. Rev. Lett., 1990, **65**, pp. 1415–1418, doi:10.1103/PhysRevLett.65.1415.

[54] A. Görlitz, T. Kinoshita, T. W. Hänsch, and A. Hemmerich, 'Realization of bichromatic optical superlattices,' Phys. Rev. A, 2001, **64**, p. 011401, doi: 10.1103/PhysRevA.64.011401.

[55] Z. Feng, S. Ebser, L. Ringena, F. Ritterbusch, and M. K. Oberthaler, 'Bichromatic force on metastable argon for atom-trap trace analysis,' Phys. Rev. A, 2017, **96**, p. 013424, doi:10.1103/PhysRevA.96.013424.

[56] S. Chu, M. G. Prentiss, A. E. Cable, and J. E. Bjorkholm, in W. Persson and S. Svanberg, editors, 'Laser Spectroscopy VII, Proceedings of the Eighth International Conference, Are, Sweden, June 22–26, 1987,' Springer, Berlin/Heidelberg, 1987 .

[57] T. Walker, D. Hoffmann, P. Feng, and R. Williamson, 'A vortex-force atom trap,' Physics Letters A, 1992, **163**(4), pp. 309–312, ISSN 0375-9601, doi: https://doi.org/10.1016/0375-9601(92)91017-L.

[58] H. J. Metcalf and P. van derStraten, 'Laser cooling and trapping of atoms,' J. Opt. Soc. Am. B, 2003, **20**(5), pp. 887–908, doi:10.1364/JOSAB.20.000887.

[59] A. Dubietis, G. Jonušauskas, and A. Piskarskas, 'Powerful femtosecond pulse generation by chirped and stretched pulse parametric amplification in bbo crystal,' Optics Communications, 1992, **88**(4), pp. 437–440, ISSN 0030-4018, doi: https://doi.org/10.1016/0030-4018(92)90070-8.

[60] W. Li, C. Peng, L. Xu, L. Yu, and X. Liang, 'Optimizing the performance of non-collinear optical parametric chirped pulse amplification via multi-pass structure based on two geometry configurations,' Opt. Express, 2017, **25**(24), pp. 30672–30685, doi: 10.1364/OE.25.030672.

[61] P. Eckle, A. N. Pfeiffer, C. Cirelli, A. Staudte, R. Dorner, H. G. Muller, M. Buttiker, and U. Keller, 'Attosecond ionization and tunneling delay time measurements in helium,' Science, 2008, **322**(5907), pp. 1525–1529, doi:10.1126/science.1163439.

[62] A. N. Pfeiffer, C. Cirelli, M. Smolarski, D. Dimitrovski, M. Abu-samha, L. B. Madsen, and U. Keller, 'Attoclock reveals natural coordinates of the laser-induced tunnelling current flow in atoms,' Nature Physics, 2011, **8**(1), pp. 76–80, doi: 10.1038/nphys2125.

[63] A. S. Landsman, M. Weger, J. Maurer, R. Boge, A. Ludwig, S. Heuser, C. Cirelli, L. Gallmann, and U. Keller, 'Ultrafast resolution of tunneling delay time,' Optica, 2014, **1**(5), p. 343, doi:10.1364/optica.1.000343.

[64] N. Camus, E. Yakaboylu, L. Fechner, M. Klaiber, M. Laux, Y. Mi, K. Z. Hatsagortsyan, T. Pfeifer, C. H. Keitel, and R. Moshammer, 'Experimental evidence for quantum tunneling time,' Physical Review Letters, 2017, **119**(2), p. 023201, doi:10.1103/physrevlett.119.023201.

[65] U. S. Sainadh, H. Xu, X. Wang, A. Atia-Tul-Noor, W. C. Wallace, N. Douguet, A. Bray, I. Ivanov, K. Bartschat, A. Kheifets, R. T. Sang, and I. V. Litvinyuk, 'Attosecond angular streaking and tunnelling time in atomic hydrogen,' Nature, 2019, **568**(7750), pp. 75–77, doi:10.1038/s41586-019-1028-3.

[66] A. S. Kheifets, 'The attoclock and the tunneling time debate,' Journal of Physics B: Atomic, Molecular and Optical Physics, 2020, **53**(7), p. 072001, doi:10.1088/1361-6455/ab6b3b.

[67] U. S. Sainadh, R. T. Sang, and I. V. Litvinyuk, 'Attoclock and the quest for tunnelling time in strong-field physics,' Journal of Physics: Photonics, 2020, **2**(4), p. 042002, doi:10.1088/2515-7647/aba009.

[68] M. Bashkansky, P. H. Bucksbaum, and D. W. Schumacher, 'Asymmetries in above-threshold ionization,' Physical Review Letters, 1988, **60**(24), pp. 2458–2461, doi: 10.1103/physrevlett.60.2458.

[69] L. Keldysh, 'Ionization in the field of a strong electromagnetic wave,' JETP, 1965, **20**(5), p. 1307.

[70] F. H. M. Faisal, 'Multiple absorption of laser photons by atoms,' Journal of Physics B: Atomic and Molecular Physics, 1973, **6**(4), pp. L89–L92, doi:10.1088/0022-3700/6/4/011.

[71] H. R. Reiss, 'Effect of an intense electromagnetic field on a weakly bound system,' Physical Review A, 1980, **22**(5), pp. 1786–1813, doi:10.1103/physreva.22.1786.

[72] P. Lambropoulos and X. Tang, 'Comment on "asymmetries in above-threshold ionization",' Physical Review Letters, 1988, **61**(21), pp. 2506–2506, doi: 10.1103/physrevlett.61.2506.

[73] H. G. Muller, G. Petite, and P. Agostini, 'Comment on "asymmetries in above-threshold ionization",' Physical Review Letters, 1988, **61**(21), pp. 2507–2507, doi: 10.1103/physrevlett.61.2507.

[74] G. G. Paulus, F. Zacher, H. Walther, A. Lohr, W. Becker, and M. Kleber, 'Above-threshold ionization by an elliptically polarized field: Quantum tunneling interferences and classical dodging,' Physical Review Letters, 1998, **80**(3), pp. 484–487, doi:10.1103/physrevlett.80.484.

[75] G. G. Paulus, F. Grasbon, A. Dreischuh, H. Walther, R. Kopold, and W. Becker, 'Above-threshold ionization by an elliptically polarized field: Interplay between electronic quantum trajectories,' Physical Review Letters, 2000, **84**(17), pp. 3791–3794, doi:10.1103/physrevlett.84.3791.

[76] Z.-M. Wang and D. S. Elliott, 'Determination of cross sections and continuum phases of rubidium through complete measurements of atomic multiphoton ionization,' Physical Review Letters, 2000, **84**(17), pp. 3795–3798, doi: 10.1103/physrevlett.84.3795.

[77] F. Dulieu, C. Blondel, and C. Delsart, 'Multiphoton angular distributions with elliptically polarized light. i. analytic ellipticity dependence of photoelectron distributions in the polarization plane,' Journal of Physics B: Atomic, Molecular and Optical Physics, 1995, **28**(17), pp. 3845–3859, doi:10.1088/0953-4075/28/17/021.

[78] Z.-M. Wang and D. S. Elliott, 'Complete measurements of two-photon ionization of atomic rubidium using elliptically polarized light,' Phys. Rev. A, 2000, **62**, p. 053404, doi:10.1103/PhysRevA.62.053404.

[79] J. Hofbrucker, A. Volotka, and S. Fritzsche, 'Maximum elliptical dichroism in atomic two-photon ionization,' Physical Review Letters, 2018, **121**(5), doi: 10.1103/physrevlett.121.053401.

[80] R. Taïeb, V. Véniard, A. Maquet, N. L. Manakov, and S. I. Marmo, 'Circular dichroism from unpolarized atoms in multiphoton multicolor ionization,' Physical Review A, 2000, **62**(1), doi:10.1103/physreva.62.013402.

[81] A. Leredde, X. Fléchard, A. Cassimi, D. Hennecart, and B. Pons, 'High-resolution probe of coherence in low-energy charge exchange collisions with oriented targets,' Physical Review Letters, 2013, **111**(13), p. 133201, doi: 10.1103/physrevlett.111.133201.

[82] M. Meyer, A. N. Grum-Grzhimailo, D. Cubaynes, Z. Felfli, E. Heinecke, S. T. Manson, and P. Zimmermann, 'Magnetic dichroism in k-shell photoemission from laser excited li atoms,' Phys. Rev. Lett., 2011, **107**, p. 213001, doi: 10.1103/PhysRevLett.107.213001.

[83] A. Harth, C. Guo, Y.-C. Cheng, A. Losquin, M. Miranda, S. Mikaelsson, C. M. Heyl, O. Prochnow, J. Ahrens, U. Morgner, A. L'Huillier, and C. L. Arnold, 'Compact 200 kHz HHG source driven by a few-cycle OPCPA,' Journal of Optics, 2017, **20**(1), p. 014007, doi:10.1088/2040-8986/aa9b04.

[84] R. Hubele, M. Schuricke, J. Goullon, H. Lindenblatt, N. Ferreira, A. Laforge, E. Brühl, V. L. B. deJesus, D. Globig, A. Kelkar, D. Misra, K. Schneider, M. Schulz, M. Sell, Z. Song, X. Wang, S. Zhang, and D. Fischer, 'Electron and recoil ion momentum imaging with a magneto-optically trapped target,' Review of Scientific Instruments, 2015, **86**(3), p. 033105, doi:10.1063/1.4914040.

[85] D. Fischer, 'Recoil ion momentum spectroscopy with laser-cooled targets,' 2019, pp. 103–156, doi:10.1515/9783110580297-006.

[86] B. J. Albright, K. Bartschat, and P. R. Flicek, 'Core potentials for quasi-one-electron systems,' Journal of Physics B: Atomic, Molecular and Optical Physics, 1993, **26**(3), pp. 337–344, doi:10.1088/0953-4075/26/3/008.

[87] M. Schuricke, G. Zhu, J. Steinmann, K. Simeonidis, I. Ivanov, A. Kheifets, A. N. Grum-Grzhimailo, K. Bartschat, A. Dorn, and J. Ullrich, 'Strong-field ionization of lithium,' Physical Review A, 2011, **83**(2), doi:10.1103/physreva.83.023413.

[88] E. Ghanbari-Adivi, D. Fischer, N. Ferreira, J. Goullon, R. Hubele, A. LaForge, M. Schulz, and D. Madison, 'Comparison of experimental and theoretical fully differential cross sections for single ionization of the $2s$ and $2p$ states of li ions,' Phys. Rev. A, 2016, **94**, p. 022715, doi:10.1103/PhysRevA.94.022715.

[89] E. Ghanbari-Adivi, D. Fischer, N. Ferreira, J. Goullon, R. Hubele, A. LaForge, M. Schulz, and D. Madison, 'Comparison of experimental and theoretical fully differential cross sections for single ionization of the $2s$ and $2p$ states of li by li2 ions,' Journal of Physics B: Atomic, Molecular and Optical Physics, 2017, **50**(21), p. 215202, doi:10.1088/1361-6455/aa8dd2.

[90] T. Young, 'On the theory of light and colours,' Philosophical Transactions of the Royal Society of London, 1802, **92**, p. 12.

[91] C. J. Davisson and L. H. Germer, 'Reflection of electrons by a crystal of nickel,' Proceedings of the National Academy of Sciences, 1928, **14**(4), pp. 317–322, doi: 10.1073/pnas.14.4.317.

[92] C. Jönsson, 'Elektroneninterferenzen an mehreren künstlich hergestellten feinspalten,' Zeitschrift für Physik, 1961, **161**(4), pp. 454–474, doi:10.1007/bf01342460.

[93] D. W. Keith, C. R. Ekstrom, Q. A. Turchette, and D. E. Pritchard, 'An interferometer for atoms,' Physical Review Letters, 1991, **66**(21), pp. 2693–2696, doi: 10.1103/physrevlett.66.2693.

[94] M. Arndt, O. Nairz, J. Vos-Andreae, C. Keller, G. van derZouw, and A. Zeilinger, 'Wave–particle duality of c60 molecules,' Nature, 1999, **401**(6754), pp. 680–682, doi:10.1038/44348.

[95] L. de Broglie, 'Thèse de doctorat (masson, paris, 1924),' J. Physique (serie 6), 1927, **VIII**, p. 225.

[96] H. Feshbach, 'Unified theory of nuclear reactions,' Annals of Physics, 1958, **5**(4), pp. 357–390, doi:10.1016/0003-4916(58)90007-1.

[97] U. Fano, 'Effects of configuration interaction on intensities and phase shifts,' Physical Review, 1961, **124**(6), pp. 1866–1878, doi:10.1103/physrev.124.1866.

[98] G. J. Schulz, 'Resonances in electron impact on atoms,' Reviews of Modern Physics, 1973, **45**(3), pp. 378–422, doi:10.1103/revmodphys.45.378.

[99] C. Chin, R. Grimm, P. Julienne, and E. Tiesinga, 'Feshbach resonances in ultracold gases,' Reviews of Modern Physics, 2010, **82**(2), pp. 1225–1286, doi: 10.1103/revmodphys.82.1225.

[100] N. Stolterfoht, B. Sulik, V. Hoffmann, B. Skogvall, J. Y. Chesnel, J. Rangama, F. Frémont, D. Hennecart, A. Cassimi, X. Husson, A. L. Landers, J. A. Tanis, M. E. Galassi, and R. D. Rivarola, 'Evidence for interference effects in electron emission fromH2colliding with60mev/uKr34 ions,' Physical Review Letters, 2001, **87**(2), p. 023201, doi:10.1103/physrevlett.87.023201.

[101] D. Misra, U. Kadhane, Y. P. Singh, L. C. Tribedi, P. D. Fainstein, and P. Richard, 'Interference effect in electron emission in heavy ion collisions withH2detected by comparison with the measured electron spectrum from atomic hydrogen,' Physical Review Letters, 2004, **92**(15), p. 153201, doi:10.1103/physrevlett.92.153201.

[102] K. N. Egodapitiya, S. Sharma, A. Hasan, A. C. Laforge, D. H. Madison, R. Moshammer, and M. Schulz, 'Manipulating atomic fragmentation processes by controlling the projectile coherence,' Physical Review Letters, 2011, **106**(15), p. 153202, doi: 10.1103/physrevlett.106.153202.

[103] S. Zhang, D. Fischer, M. Schulz, A. Voitkiv, A. Senftleben, A. Dorn, J. Ullrich, X. Ma, and R. Moshammer, 'Two-center interferences in dielectronic transitions inH2HeCollisions,' Physical Review Letters, 2014, **112**(2), p. 023201, doi: 10.1103/physrevlett.112.023201.

[104] D. S. Milne-Brownlie, M. Foster, J. Gao, B. Lohmann, and D. H. Madison, 'Young-type interference in(e,2e)ionization ofH2,' Physical Review Letters, 2006, **96**(23), p. 233201, doi:10.1103/physrevlett.96.233201.

[105] X. Li, X. Ren, K. Hossen, E. Wang, X. Chen, and A. Dorn, 'Two-center interference in electron-impact ionization of molecular hydrogen,' Physical Review A, 2018, **97**(2), p. 022706, doi:10.1103/physreva.97.022706.

[106] H. D. Cohen and U. Fano, 'Interference in the photo-ionization of molecules,' Physical Review, 1966, **150**(1), pp. 30–33, doi:10.1103/physrev.150.30.

[107] M. Kunitski, N. Eicke, P. Huber, J. Köhler, S. Zeller, J. Voigtsberger, N. Schlott, K. Henrichs, H. Sann, F. Trinter, L. P. H. Schmidt, A. Kalinin, M. S. Schöffler, T. Jahnke, M. Lein, and R. Dörner, 'Double-slit photoelectron interference in strong-field ionization of the neon dimer,' Nature Communications, 2019, **10**(1), doi:10.1038/s41467-018-07882-8.

[108] H. Muller, 'Reconstruction of attosecond harmonic beating by interference of two-photon transitions,' Applied Physics B, 2002, **74**(S1), pp. s17–s21, doi:10.1007/s00340-002-0894-8.

[109] K. Klünder, J. M. Dahlström, M. Gisselbrecht, T. Fordell, M. Swoboda, D. Guénot, P. Johnsson, J. Caillat, J. Mauritsson, A. Maquet, R. Taïeb, and A. L'Huillier, 'Probing single-photon ionization on the attosecond time scale,' Physical Review Letters, 2011, **106**(14), p. 143002, doi:10.1103/physrevlett.106.143002.

[110] M. Isinger, R. J. Squibb, D. Busto, S. Zhong, A. Harth, D. Kroon, S. Nandi, C. L. Arnold, M. Miranda, J. M. Dahlström, E. Lindroth, R. Feifel, M. Gisselbrecht, and A. L'Huillier, 'Photoionization in the time and frequency domain,' Science, 2017, **358**(6365), pp. 893–896, doi:10.1126/science.aao7043.

[111] D. Bharti, D. Atri-Schuller, G. Menning, K. R. Hamilton, R. Moshammer, T. Pfeifer, N. Douguet, K. Bartschat, and A. Harth, 'Decomposition of the transition phase in multi-sideband schemes for reconstruction of attosecond beating by interference of two-photon transitions,' Physical Review A, 2021, **103**(2), p. 022834, doi:10.1103/physreva.103.022834.

[112] Y.-Y. Yin, C. Chen, D. S. Elliott, and A. V. Smith, 'Asymmetric photoelectron angular distributions from interfering photoionization processes,' Physical Review Letters, 1992, **69**(16), pp. 2353–2356, doi:10.1103/physrevlett.69.2353.

[113] F. Ehlotzky, 'Atomic phenomena in bichromatic laser fields,' Physics Reports, 2001, **345**(4), pp. 175–264, doi:10.1016/s0370-1573(00)00100-9.

[114] C. Brif, R. Chakrabarti, and H. Rabitz, 'Control of quantum phenomena: past, present and future,' New Journal of Physics, 2010, **12**(7), p. 075008, doi:10.1088/1367-2630/12/7/075008.

[115] L. Giannessi, E. Allaria, K. C. Prince, C. Callegari, G. Sansone, K. Ueda, T. Morishita, C. N. Liu, A. N. Grum-Grzhimailo, E. V. Gryzlova, N. Douguet, and K. Bartschat, 'Coherent control schemes for the photoionization of neon and helium in the extreme ultraviolet spectral region,' Scientific Reports, 2018, **8**(1), doi: 10.1038/s41598-018-25833-7.

[116] P.-L. He, Z.-H. Zhang, and F. He, 'Young's double-slit interference in a hydrogen atom,' Physical Review Letters, 2020, **124**(16), p. 163201, doi: 10.1103/physrevlett.124.163201.

[117] J. Pursehouse, A. J. Murray, J. Wätzel, and J. Berakdar, 'Dynamic double-slit experiment in a single atom,' Physical Review Letters, 2019, **122**(5), p. 053204, doi: 10.1103/physrevlett.122.053204.

[118] B. P. Acharya, M. Dobson, S. Dubey, K. L. Romans, A. H. N. C. D. Silva, K. Foster, O. Russ, K. Bartschat, N. Douguet, and D. Fischer, 'Magnetic dichroism in the few-photon ionization of polarized atoms,' Physical Review A, to be submitted.

[119] S. H. Autler and C. H. Townes, 'Stark effect in rapidly varying fields,' Physical Review, 1955, **100**(2), pp. 703–722, doi:10.1103/physrev.100.703.

[120] M. Pahler, C. Lorenz, E. v. Raven, J. Rüder, B. Sonntag, S. Baier, B. R. Müller, M. Schulze, H. Staiger, P. Zimmermann, and N. M. Kabachnik, 'Angle-dependent photoelectron spectroscopy of laser-aligned atoms: Li,' Phys. Rev. Lett., 1992, **68**, pp. 2285–2288, doi:10.1103/PhysRevLett.68.2285.

[121] U. Becker, 'Complete photoionisation experiments1dedicated to professor h. klein-poppen, stirling, for his 70th birthday.1,' Journal of Electron Spectroscopy and Related Phenomena, 1998, **96**(1), pp. 105 – 115, ISSN 0368-2048, doi: https://doi.org/10.1016/S0368-2048(98)00226-6.

[122] K. Godehusen, P. Zimmermann, A. Verweyen, A. von demBorne, P. Wernet, and B. Sonntag, 'A complete photoionization experiment with polarized atoms using magnetic dichroism and phase tilt measurements,' Phys. Rev. A, 1998, **58**, pp. R3371–R3374, doi:10.1103/PhysRevA.58.R3371.

VITA

Bishnu Prasad Acharya was born in Dibharna Arghakhanchi of Nepal. He completed high school in his hometown Dibharna and nearby city Sandhikharkha, Arghakhanchi. After completing high school, he moved to Butwal and Kathmandu and completed his undergraduate degree from Butwal multiple campus and Tri-Chandra campus in 2005 with physics, chemistry and mathematics on a merit-based freeship. After his bachelor's degree, he joined the Central Department of Physics Kirtipur Nepal. In his master's degree, except fundamental courses he took major courses plasma physics and solid-state physics. After completing his MS from Tribhuvan University Nepal he joined Missouri S&T as a master's student in 2013. After, MS he joined Dr. Daniel Fischer's lab as a Ph. D. student. While he was in Rolla, he greatly enjoyed his research works under the supervision of Dr. Daniel Fischer in most recent developed advanced experimental tools. He received his Doctor of Philosophy in Physics from Missouri University of Science and Technology in December 2021 under the guidance of Dr. Daniel Fischer. Bishnu worked as graduate teaching and research assistant at Physics Department of Missouri University of Science and Technology for more than six years. Also, he worked as an Assistant Professor at Nepal Engineering College Bhaktapur Nepal for six years